THE HONG KONG UNIVERSITY OF SCIENCE AND TECHNOLOGY

Final Report for Chemical Speciation of $PM_{2.5}$ Filter Samples

January 1 through December 31, 2022

(Quotation Ref. 21-02409)

Prepared by:

Prof. Jian Zhen Yu
Dr. Wing Sze Chow
Dr. Ting Zhang
Dr. Qingyan Zhang
Dr. Yee Ka Wong

Environmental Central Facility
The Hong Kong University of Science & Technology
Clear Water Bay, Kowloon, Hong Kong

Presented to:

Environmental Protection Department
The Government of the Hong Kong Special Administrative Region

December 2023

[This page was intentionally left blank.]

Table of Content

List of Figures

List of Tables

Acronyms, Abbreviations and Chemical Symbols

Ag	Silver
Al	Aluminum
AQMS	Air Quality Monitoring Station
AQO	Air Quality Objective
AQRS	Air Quality Research Site
As	Arsenic
Au	Gold
Ba	Barium
BLK	Blank
Br	Bromine
Ca	Calcium
Ca^{2+}	Calcium ion
Cd	Cadmium
Cs	Cesium
CSN	Chemical Speciation Network
Cu	Copper
CW	Central/Western
EC	Elemental carbon
ED-XRF	Energy-Dispersive X-Ray Fluorescence Spectroscopy
Eu	Europium
Fe	Iron
Ga	Gallium
He	Helium
Hf	Hafnium
Hg	Mercury
HKENB	Hong Kong Environment Bureau
HKEPD	Hong Kong Environmental Protection Department
HT	Hok Tsui
IC	Ion chromatography
IMPROVE_A	A thermal/optical carbon analysis temperature protocol
In	Indium
Ir	Iridium
K	Potassium
K^+	Potassium ion
KC	Kwai Chung
La	Lanthanum
LOD	Limit of Detection
LOQ	Limit of Quantification
Mg	Magnesium
MK	Mong Kok
Mn	Manganese
Mo	Molybdenum
Na	Sodium
Na^+	Sodium ion
Nb	Niobium
NH_4^+	Ammonium
NH_4NO_3	Ammonium nitrate
$(NH_4)_2SO_4$	Ammonium sulfate
NH_4HSO_4	Ammonium bisulfate
Ni	Nickel
NO_3^-	Nitrate
O_2	Oxygen
OC	Organic carbon
P	Phosphorus
Pb	Lead
Pd	Palladium
PM	Particulate matter

$PM_{2.5}$	Particles with aerodynamic diameter ≤2.5 µm
QA	Quality assurance
QC	Quality control
Rb	Rubidium
S	Sulfur
Sb	Antimony
Sc	Scandium
Se	Selenium
Si	Silicon
Sm	Samarium
Sn	Tin
SO_4^{2-}	Sulfate
Sr	Strontium
Ta	Tantalum
Tb	Terbium
TC	Tung Chung
Ti	Titanium
Tl	Thallium
TOR	Thermal Optical Reflectance
TOT	Thermal Optical Transmittance
TotC	Total carbon
TW	Tsuen Wan
U	Uranium
USEPA	United States Environmental Protection Agency
V	Vanadium
W	Wolfram
WB	Clear Water Bay
WHO	World Health Organization
Y	Yttrium
YL	Yuen Long
Zn	Zinc
Zr	Zirconium

[This page was intentionally left blank.]

1. Introduction

1.1 Background

The Environmental Protection Department of the Hong Kong Special Administration Region (HKEPD) put in force an updated Air Quality Objectives (AQOs) in January 2022. In the new AQOs, the concentration limit for 24-hour average $PM_{2.5}$ is set to be 50 $\mu g/m^3$ with 35 exceedance days allowed while the limit for annual average $PM_{2.5}$ is 25 $\mu g/m^3$.

The Environment and Ecology Bureau (EEB) and the HKEPD have been implementing a wide range of measures locally to reduce the air pollution. In November 2012, the Hong Kong Special Administrative Region and Guangdong Provincial Governments endorsed emission reduction targets for 2015 while in December 2017, the emission reduction targets for 2020 were set, strengthening the collaboration between Guangdong and Hong Kong to deal with the regional air pollution.

The on-going control measures aside, continuous monitoring of the air quality is necessary for the air pollution trend analysis. More specifically, the $PM_{2.5}$ chemical speciation studies would provide a better understanding on the nature and relative contributions of different emission sources that are responsible for the observed $PM_{2.5}$ levels in Hong Kong.

The HKEPD established a $PM_{2.5}$ chemical speciation network in 2000 and monitoring operations began in November 2000. Up to 2016, the HKEPD supported seven sampling sites which includes four collocated sites. In 2017, the network was reduced to five sampling sites with two collocated sites. HKUST has been supporting the HKEPD with the chemical speciation analysis of the $PM_{2.5}$ filter samples during 2011–2014 and in 2016–2017, 2019, and 2022.

This report documents the $PM_{2.5}$ measurements and data validation for a twelve-month monitoring program from January to December 2022. The data were analyzed to characterize the composition and temporal and spatial variations of $PM_{2.5}$ concentrations in Hong Kong. Trends of $PM_{2.5}$ concentration and chemical composition were established by comparing the current study to the previous 12-month $PM_{2.5}$ studies since 2000. The monitoring data can further be used to explore the source contributions and investigate hypotheses regarding the formation of $PM_{2.5}$ episodes.

1.2 Project Objectives and Task Description

The Environmental Central Facility (ENVF) at the Hong Kong University of Science and Technology (HKUST) has been contracted by the HKEPD in the analysis of $PM_{2.5}$ samples acquired over the course from January to December 2022. The objectives of this study were to:

- Determine the organic and inorganic composition of $PM_{2.5}$ and how it differs by season and proximity to different types of emission sources.
- Based on the ambient concentrations of certain tracer compounds, determine the contributions of different sources to $PM_{2.5}$ in Hong Kong.
- Investigate and understand the influences of meteorological/atmospheric conditions on $PM_{2.5}$ episodic events in Hong Kong.

- Establish inter-annual variability of $PM_{2.5}$ concentration and chemical composition in Hong Kong urban and rural areas.

The ENVF/HKUST team is responsible for:

- Receiving samples from the HKEPD and analyzing the filter samples for gravimetric mass and for an array of chemical constituents, including elements, soluble anions and cations, and carbonaceous material.
- Assembling validated sets of data from the analyses and preparing data files, which will be entered into the HKEPD $PM_{2.5}$ speciation database.

1.3 Technical Approach

During the sampling period from January to December 2022, 24-hour $PM_{2.5}$ filter samples were acquired once every six days from the roadside-source-dominated Mong Kok (MK) Air Quality Monitoring Station (AQMS), the urban Tsuen Wan (TW) and Kwai Chung (KC) AQMSs, the new town Yuen Long (YL) AQMS, and the suburban Clear Water Bay (WB) Air Quality Research Site (AQRS) which is located on the campus of the Hong Kong University of Science and Technology. Three BGI PQ200 samplers (BGI Incorporated, Model PQ200, Butler, NJ, USA) were placed at MK and WB sites respectively and two BGI PQ200 samplers were placed at TW, KC and YL sites respectively to obtain $PM_{2.5}$ samples on both Teflon-membrane and quartz fiber 47-mm filters. All sampled Teflon-membrane and quartz fiber filters were analyzed for mass by gravimetric analysis by HKEPD's contractor and then subjected to a suite of chemical analyses, including 1) determination of elements for atomic number ranging from 11 (sodium) to 92 (uranium) using Energy-Dispersive X-Ray Fluorescence (ED-XRF) Spectroscopy; 2) determination of chloride, nitrate, sulfate, sodium, ammonium, and potassium using Ion Chromatography (IC); and 3) determination of organic carbon (OC), elemental carbon (EC), total carbon (TotalC), individual thermal fractions for OC, EC, and pyrolyzed carbon on quartz fiber filters using Thermal Optical Transmittance (TOT) and Thermal Optical Reflectance (TOR) methods coupled with IMPROVE_A protocol.

2. Sampling Network

2.1 Ambient $PM_{2.5}$ Monitoring Network

24-hour $PM_{2.5}$ filter samples were collected at four AQMSs and one AQRS in Hong Kong once every six days from January to December 2022. The five sampling sites are shown in Figure 1, representing roadside (MK), urban (TW and KC), new town (YL), and suburban (WB) areas. The names, codes, locations, and descriptions of the individual sites are listed in Table 1.

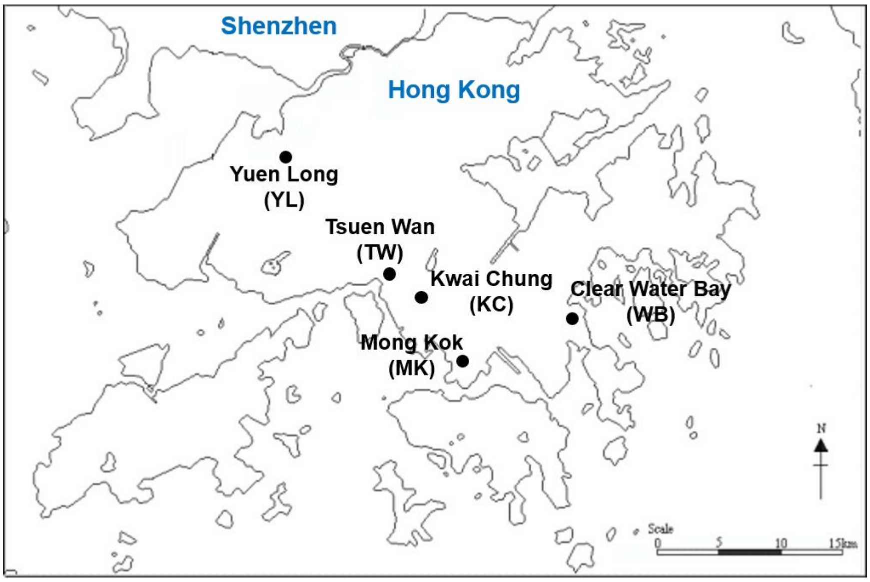

Figure 1. Monitoring sites in Hong Kong $PM_{2.5}$ speciation network in 2022.

Table 1. Descriptions of the air quality monitoring sites

Site Name	Site Code	Site Location	Site Description
Mong Kok	MK	Junction of Lai Chi Kok Road and Nathan Road, Kowloon	Urban roadside in mixed residential/commercial area with heavy traffic and surrounded by many tall buildings
Clear Water Bay	WB	Rooftop of a pump house next to Air Quality Research Supersite, HKUST Campus, Clear Water Bay	Clean rural area with little residential and commercial development on the east coast of Sai Kung
Tsuen Wan	TW	Rooftop of Princess Alexandra Community Center, 60 Tai Ho Road, New Territories	Urban, densely populated, residential site with mixed commercial and industrial developments. Located northwest of the MK site
Yuen Long	YL	Rooftop of Yuen Long District Branch Office Building, 269 Castle Peak Road, New Territories	Residential town, about 15 km southwest of Shenzhen
Kwai Chung	KC	Rooftop of the Kwai Chung Police Station, 999 Kwai Chung Road, New Territories	Urban, densely populated residential site with mixed commercial and industrial developments, close to the Kwai Tsing Container Terminals

2.2 Ambient $PM_{2.5}$ Measurements

A total of 12 samplers were employed to obtain $PM_{2.5}$ samples around Hong Kong. The detailed arrangement of the samplers is described in Table 2.

Table 2. Arrangement of the air samplers in the monitoring sites

Location	Sampler Brand	No. of Samplers	Collocated Samples
MK AQMS	BGI PQ200	3	Teflon Filters
WB AQRS	BGI PQ200	3	Quartz Fiber Filters
TW AQMS	BGI PQ200	2	
YL AQMS	BGI PQ200	2	
KC AQMS	BGI PQ200	2	

Each air sampler was equipped with an $PM_{2.5}$ inlet with Very Sharp Cut Cyclone. The samplings were conducted at a flow rate of 16.7 L/min. At this flow rate, a nominal volume of approx. 24.0 m^3 of ambient air would be sampled over a 24-hour period. The air samplers were configured to take either a Teflon-membrane filter or a quartz fiber filter. For this study, the following filters were chosen: 1) Whatman (Clifton, NJ, USA), $PM_{2.5}$ membrane, PTFE, 46.2 mm with support ring (#7592104); and 2) Pall Life Sciences (Ann Arbor, MI, USA), 2500QAT-UP, 47 mm, Tissuquartz™ filters (#7202D).

The air samplers were operated and maintained by HKEPD's contractor, AECOM Asia Company Limited, throughout the study period. The ENVF/HKUST team was responsible for pre- and post-sampling procedures required for quality assurance and sample preservation. ENVF/HKUST team was also responsible for the chemical analysis and gravimetric analysis on both filter types before and after sampling.

The collected Teflon-membrane filters were used for gravimetric analysis for $PM_{2.5}$ mass concentrations and elemental analysis (for more than 40 elements with atomic number ranging from 11 to 92) by ED-XRF [Watson et al., 1999]. The collected quartz fiber filters were analyzed for mass concentrations by gravimetry, for carbon contents by multiple thermal optical methods, and for chloride (Cl^-), nitrate (NO_3^-), sulfate (SO_4^{2-}), water-soluble sodium (Na^+), ammonium (NH_4^+), and water-soluble potassium (K^+) by IC.

A major uncertainty in determining carbon concentrations lies in the differentiation of organic and elemental carbon during analysis. EC is defined as the carbon that evolves after the detected optical signal attains the initial value prior to commencement of heating and the rest of the carbon is considered to be OC [Chow et al., 1993; Birch and Cary, 1996]. The split of OC and EC in the thermal analysis depends on several parameters including temperature setpoints, temperature ramping rates, residence time at each setpoint, combustion atmospheres, and optical signal used. Heating in an inert atmosphere causes certain OC to pyrolyze or char, inflating the EC in the sample. The extent of pyrolysis is dependent on thermal/temperature protocols. A laser is used to correct for pyrolitically-produced EC by monitoring changes in filter darkness during the thermal evolution process by detecting either filter transmittance (thermal/optical transmittance [TOT] method) or reflectance (thermal/optical reflectance [TOR] method). However, this introduces another problem related to inner/near-surface filter pyrolysis. It is found that pyrolysis occurs both within filter and on the filter surface. TOT method measures light transmittance which goes through the filter and is more likely influenced by the inner filter char while TOR method is more influenced by the charring of near-surface deposit. Results obtained with the two methods are compared and evaluated in Section 3.3.4.

2.3 Sample Delivery and Filter Conditions

A total of 870 filter samples including 433 Teflon filters and 437 quartz fiber filters were received. The valid sampling dates are summarized in Table 3. In 2022, there were 61 valid sampling events at MK, WB, YL, and KC sites, and 60 at TW site. In addition, there is one set of field blank filters each month at each of the five sampling sites.

Table 3. Valid sampling dates for the $PM_{2.5}$ samples in 2022 (Quotation Ref. 21-02409)

Sampling Dates					
January 2022	February 2022	March 2022	April 2022	May 2022	June 2022
220105	220204	220306	220405	220505	220604
220111	220210	220312	220411	220511	220610
220117 w/BLK	220216 w/BLK	220318 w/BLK	220417 w/BLK	220517 w/BLK	220616 w/BLK
220123	220222	220324	220423	220523	220622
220129	220228	220330	220429	220529	220628
July 2022	August 2022	September 2022	October 2022	November 2022	December 2022
220704	220803	220902	221002	221107	221201
220710	220809	220908	221008	221113 w/BLK	221207
220716 w/BLK	220815 w/BLK	220914 w/BLK	221014 w/BLK	221116[b]	221211 w/BLK[c]
220722	220821	220920	221020	221119	221221[c]
220728	220827	220926		221122[b]	221225
220731[a]				221125	

[a] Make-up sampling performed at TW site.
[b] Make-up sampling performed at MK site.
[c] Due to Tsuen Wan site re-roofing work, the sampling date from 13 and 19 December, 2022 changed to the 11 December and 21 December, 2022, respectively.

It is noted that a total of 30 filter samples were voided. The corresponding sample ID, filter ID, and a brief account for voiding the sample are provided in Table 4.

Table 4. Invalid $PM_{2.5}$ filter sample identified during field validation in 2022 (Quotation Ref. 21-0249)

Sample ID	Filter ID	Cause
MK220405SF02T	T0010109	Filter found broken
TW220523SF02T	T0010172	Sampling pump malfunction
TW220610SF02T	T0010190	Two pinholes observed
TW220722SF01Q	Q0010244	Sampler failure
MK221026SF01Q	Q0010361	Voided
WB221026SF01Q	Q0010362	Voided
WB221026PF03Q	Q0010363	Voided
TW221026SF01Q	Q0010364	Voided
YL221026SF01Q	Q0010365	Voided
KC221026SF01Q	Q0010366	Voided
MK221101SF01Q	Q0010367	Voided
WB221101SF01Q	Q0010368	Voided
WB221101PF03Q	Q0010369	Voided
TW221101SF01Q	Q0010370	Voided
YL221101SF01Q	Q0010371	Voided
KC221101SF01Q	Q0010372	Voided
TW220722SF02T	T0010244	Sampler failure
TW220803SF02T	T0010262	Sampler failure
MK221026SF02T	T0010361	Voided
MK221026PF03T	T0010362	Voided
WB221026SF02T	T0010363	Voided
TW221026SF02T	T0010364	Voided
YL221026SF02T	T0010365	Voided
KC221026SF02T	T0010366	Voided
MK221101SF02T	T0010367	Voided
MK221101PF03T	T0010368	Voided
WB221101SF02T	T0010369	Voided
TW221101SF02T	T0010370	Voided
YL221101SF02T	T0010371	Voided
KC221101SF02T	T0010372	Voided

For the voided samples collected on 26th October and 1st November, the chemical information was incomplete since the collocated Teflon samples failed to meet the EPD proposed criteria for $PM_{2.5}$ mass comparison.

For the one voided samples at MK site, the chemical information was incomplete since only one quartz filter sample was collected and no valid Teflon filter sample was available at this site in these sampling events.

For the three voided samples at TW sites, the chemical information was incomplete since only one quartz fiber filter sample was collected and no valid Teflon filter sample was available at these sites in these sampling events. While for the two voided samples at TW sites on 22nd July, the incomplete chemical information was resulted because no valid Teflon and quartz filter sample was available.

3. Database and Data Validation

3.1 Data File Preparation

An electronic database for the analytical results is established for Hong Kong $PM_{2.5}$ data archive. Detailed data processing and data validation are documented in Section 3.3. The data are available on Compact Disc in the format of Microsoft Excel spreadsheets for convenient distribution to data users. The contents of the final data files are summarized in Table 5.

Table 5. Summary of data files for the 2022 $PM_{2.5}$ study (EPD Quotation Ref. 21-02409) in Hong Kong

Category	Database File	File Description
I. DATABASE DOCUMENTATION		
	21-02409_ID.xls	Defines the field sample names, measurement units, and formats used in the database file
II. MASS AND CHEMICAL DATA		
	21-02409_PM2.5.xls	Contains $PM_{2.5}$ mass data and chemical data for samples collected by $PM_{2.5}$ air samplers at five sites once every six days in 2022
III. DATABASE VALIDATION		
	21-02409_FLAG.xls	Contains both field sampling and chemical analysis data validation flags

3.2 Measurement and Analytical Specifications

The measurement/analysis methods are described in Section 1.3 and every measurement consists of 1) a value; 2) a precision (uncertainty), and 3) a validity statement. The values are obtained by different analysis methods. The precisions are estimated through standard testing, blank analysis, and replicate analysis. The validity of each measurement is indicated by appropriate flagging in the database, while the validity of chemical analysis results are evaluated by data validation described in Section 3.3.

A total of 61 sets of ambient $PM_{2.5}$ samples and 12 sets of field blanks were received during this study. Collocated sampling was conducted at two out of five sites and the collocated samples were used for data validation purpose. All of the 870 samples (726 $PM_{2.5}$ samples and 144 field blanks) received are considered valid after Level I data validation. All the samples were submitted for comprehensive chemical analyses.

3.2.1 Precision Calculations and Error Propagation

Measurement precisions are propagated from precisions of volumetric measurements, chemical composition measurements, and field blank variability using the methods of Bevington [1969] and Watson et al. [2001]. The following equations are used to calculate the precision associated with filter-based measurements:

$$C_i = \frac{M_i - B_i}{V} \quad (1)$$

$$V = Q \times T \quad (2)$$

$$B_i = \frac{1}{n}\sum_{j=1}^{n} B_{ij} \qquad for\ B_i > \sigma_{B_i} \quad (3)$$

$$B_i = 0 \qquad for\ B_i \le \sigma_{B_i} \quad (4)$$

$$\sigma_{B_i} = STD_{B_i} = \left[\frac{1}{n-1}\sum_{j=1}^{n}\left(B_{ij} - B_i\right)^2\right]^{\frac{1}{2}} \qquad for\ STD_{B_i} > SIG_{B_i} \quad (5)$$

$$\sigma_{B_i} = SIG_{B_i} = \left[\frac{1}{n}\sum_{j=1}^{n}\left(\sigma_{B_{ij}}\right)^2\right]^{\frac{1}{2}} \qquad for\ STD_{B_i} \le SIG_{B_i} \quad (6)$$

$$\frac{\sigma_V}{V} = 0.05 \quad (7)$$

$$\sigma_{C_i} = \left[\frac{\sigma_{Mi}^2 + \sigma_{Bi}^2}{V^2} + \frac{\sigma_V^2 (M_i - B_i)^2}{V^4}\right]^{\frac{1}{2}} \quad (8)$$

Where:

B_i	= average amount of species i on field blanks
B_{ij}	= the amount of species i found on field blank j
C_i	= the ambient concentration of species i
Q	= flow rate throughout sampling period
M_i	= amount of species i on the substrate
n	= total number of samples in the sum
SIG_{Bi}	= the root mean square error (RMSE), the square root of the averaged sum of the squared σ_{Bij}
STD_{Bi}	= standard deviation of the blank
σ_{Bi}	= blank precision for species i
σ_{Bij}	= precision of the species i found on field blank j
σ_{Ci}	= propagated precision for the concentration of species i
σ_{Mi}	= precision of amount of species i on the substrate
σ_V	= precision of sample volume
T	= sample duration
V	= volume of air sampled

The uncertainty of the measured value and the average uncertainty of the field blanks for each species are used to propagate the overall precision for each blank subtracted concentration value. The final value is propagated by taking the square root of the sum of the squares of the calculated uncertainty and the average field blank uncertainty for each measurement.

3.2.2 Analytical Specifications

The precisions (σ_{Mi}) were determined from duplicate analysis of samples. When duplicate sample analysis is made, the range of results, R, is nearly as efficient as the standard deviation since two measures differ by a constant ($1.128\sigma_{Mi} = R$).

Table 6. Field blank concentrations of $PM_{2.5}$ samples collected at MK, WB, TW, YL, and KC sites during the study period (2022) in Hong Kong

	Amount on µg/47-mm filter					
Species	**Total No. of Blanks**	**Field Blank Std. Dev. (STD_{Bi})**	**Root Mean Squared Blank Precision (SIG_{Bi})**	**Blank Precision (σ_{Bi})**	**Average Field Blank**	**Blank Subtracted (B_i)**
Na^+	72	0.105	0.103	0.105	-0.306	0.000
NH_4^+	72	0.504	1.369	1.369	0.061	0.000
K^+	72	0.174	0.471	0.471	-0.157	0.000
Cl^-	72	0.103	0.317	0.317	0.443	0.443
NO_3^-	72	0.313	0.525	0.525	2.088	2.088
SO_4^{2-}	72	0.279	0.680	0.680	-1.259	0.000
OC1	72	1.214	0.117	1.214	3.301	3.301
OC2	72	2.433	0.119	2.433	5.464	5.464
OC3	72	3.375	0.231	3.375	9.051	9.051
OC4	72	0.854	0.089	0.854	1.066	1.066
EC1	72	0.651	0.060	0.651	0.301	0.000
EC2	72	0.738	0.061	0.738	0.495	0.000
EC3	72	0.812	0.056	0.812	0.480	0.000
PyC_TOR	72	0.882	0.049	0.882	0.320	0.000
OC_TOR	72	7.932	0.498	7.932	19.203	19.203
EC_TOR	72	1.670	0.116	1.670	0.964	0.000
TotC	72	8.840	0.577	8.840	20.167	20.167
PyC_TOT	72	1.943	0.057	1.943	1.075	0.000
OC_TOT	72	8.702	0.512	8.702	19.958	19.958
EC_TOT	72	0.644	0.087	0.644	0.209	0.000
Na	72	0.087	0.237	0.237	-0.015	0.000
Mg	72	0.276	0.438	0.438	-0.052	0.000
Al	72	0.128	0.283	0.283	-0.151	0.000

Species	Amount on µg/47-mm filter					
	Total No. of Blanks	Field Blank Std. Dev. (STD_{Bi})	Root Mean Squared Blank Precision (SIG_{Bi})	Blank Precision (σ_{Bi})	Average Field Blank	Blank Subtracted (B_i)
Si	72	0.596	0.629	0.629	-0.115	0.000
P	72	0.023	0.057	0.057	-0.021	0.000
S	72	0.000	0.072	0.072	0.000	0.000
Cl	72	0.016	0.072	0.072	-0.012	0.000
K	72	0.001	0.043	0.043	0.000	0.000
Ca	72	0.020	0.068	0.068	-0.006	0.000
Sc	72	0.092	0.172	0.172	-0.069	0.000
Ti	72	0.009	0.040	0.040	0.006	0.000
V	72	0.007	0.014	0.014	0.002	0.000
Cr	72	0.020	0.180	0.180	-0.020	0.000
Mn	72	0.041	0.122	0.122	0.023	0.000
Fe	72	0.061	0.737	0.737	0.015	0.000
Co	72	0.014	0.032	0.032	-0.001	0.000
Ni	72	0.016	0.032	0.032	-0.006	0.000
Cu	72	0.017	0.086	0.086	0.013	0.000
Zn	72	0.018	0.050	0.050	-0.004	0.000
Ga	72	0.069	0.194	0.194	-0.052	0.000
Ge	72	0.370	1.194	1.194	0.175	0.000
As	72	0.000	0.613	0.613	0.000	0.000
Se	72	0.000	0.613	0.613	0.000	0.000
Br	72	0.010	0.613	0.613	0.004	0.000
Rb	72	0.016	0.032	0.032	0.009	0.000
Sr	72	0.019	0.047	0.047	0.005	0.000
Y	72	0.013	0.043	0.043	0.012	0.000
Zr	72	0.046	0.111	0.111	-0.009	0.000
Nb	72	0.035	0.093	0.093	-0.027	0.000
Mo	72	0.037	0.068	0.068	0.005	0.000
Rh	72	0.055	0.122	0.122	0.034	0.000
Pd	72	0.112	0.133	0.133	-0.014	0.000
Ag	72	0.038	0.115	0.115	0.023	0.000
Cd	72	0.053	0.115	0.115	-0.015	0.000
In	72	0.110	0.144	0.144	-0.073	0.000
Sn	72	0.088	0.230	0.230	0.050	0.000

Species	Amount on µg/47-mm filter					
	Total No. of Blanks	Field Blank Std. Dev. (STD_{Bi})	Root Mean Squared Blank Precision (SIG_{Bi})	Blank Precision (σ_{Bi})	Average Field Blank	Blank Subtracted (B_i)
Sb	72	0.141	0.187	0.187	0.059	0.000
Te	72	0.108	0.313	0.313	-0.036	0.000
I	72	0.131	0.353	0.353	0.035	0.000
Cs	72	0.276	0.684	0.684	-0.315	0.000
Ba	72	0.338	0.947	0.947	-0.234	0.000
La	72	0.370	0.986	0.986	-0.277	0.000
Ce	72	0.007	0.043	0.043	0.002	0.000
Sm	72	0.026	0.075	0.075	0.005	0.000
Eu	72	0.075	0.190	0.190	-0.066	0.000
Tb	72	0.019	0.072	0.072	0.006	0.000
Hf	72	0.114	0.338	0.338	-0.106	0.000
Ta	72	0.103	1.761	1.761	0.018	0.000
W	72	0.790	0.257	0.790	-0.183	0.000
Ir	72	0.023	0.149	0.149	0.008	0.000
Au	72	0.000	0.149	0.149	0.000	0.000
Hg	72	0.025	0.149	0.149	0.003	0.000
Tl	72	0.019	0.149	0.149	0.008	0.000
Pb	72	0.040	0.041	0.041	-0.003	0.000
U	72	0.055	0.144	0.144	0.087	0.000

The analytical specifications for the 24-hour $PM_{2.5}$ measurements obtained during the study are summarized in Table 7. Limits of detection (LOD) and limits of quantitation (LOQ) are given in Table 7. The LOD of an analyte may be described as the concentration that gives an instrument signal significantly different from the "blank" or "background" signal. In this study LOD is defined as the concentration at which instrument response equals three times the standard deviation of the concentrations of a low-level standard. As a further limit, the LOQ is regarded as the lower limit for precise quantitative measurements and is defined as a concentration corresponding to ten times the standard deviation of the concentration measurement of the low-level standard. Both the LODs and LOQs are in the unit of µg/m^3 assuming the effective sampling area of the 47-mm filter is 11.98 cm^2 and the sampling volume is 24 m^3.

Table 7. Analytical specifications of 24-hour $PM_{2.5}$ measurements at MK, WB, TW, YL, and KC sites during the study period (2019) in Hong Kong

Species	Analytical Method	LOD, µg/m³	LOQ, µg/m³	No. of Valid Values	No. > LOD	% > LOD	No. > LOQ	% > LOQ
Na^+	IC	0.004	0.014	365	360	99%	355	97%
NH_4^+	IC	0.057	0.190	365	365	100%	355	97%
K^+	IC	0.020	0.065	365	345	95%	239	65%
Cl^-	IC	0.013	0.044	365	310	85%	196	54%
NO_3^-	IC	0.021	0.069	365	360	99%	352	96%
SO_4^{2-}	IC	0.028	0.093	365	365	100%	362	99%
OC1	TOR	0.070	0.234	365	162	44%	44	12%
OC2	TOR	0.097	0.323	365	365	100%	351	96%
OC3	TOR	0.173	0.576	365	362	99%	297	81%
OC4	TOR	0.078	0.261	365	363	99%	341	93%
EC1	TOR	0.057	0.189	365	363	99%	356	98%
EC2	TOR	0.057	0.189	365	358	98%	198	54%
EC3	TOR	0.041	0.138	365	78	21%	6	2%
PyC_TOR	TOR	0.045	0.150	365	361	99%	339	93%
OC_TOR	TOR	0.394	1.312	365	363	99%	331	91%
EC_TOR	TOR	0.108	0.359	365	359	98%	338	93%
TotC	TOR	0.475	1.583	365	363	99%	337	92%
PyC_TOT	TOT	0.050	0.168	365	362	99%	338	93%
OC_TOT	TOT	0.405	1.350	365	363	99%	328	90%
EC_TOT	TOT	0.082	0.274	365	361	99%	348	95%
Na	XRF	0.025	0.082	360	357	99%	293	81%
Mg	XRF	0.045	0.151	360	319	89%	79	22%
Al	XRF	0.029	0.098	360	305	85%	153	43%
Si	XRF	0.065	0.217	360	299	83%	131	36%
P	XRF	0.006	0.020	360	1	0%	0	0%
S	XRF	0.007	0.025	360	360	100%	360	100%
Cl	XRF	0.007	0.025	360	320	89%	167	46%
K	XRF	0.004	0.015	360	360	100%	359	100%
Ca	XRF	0.007	0.024	360	358	99%	339	94%
Sc	XRF	0.018	0.060	360	0	0%	0	0%
Ti	XRF	0.004	0.014	360	274	76%	45	13%

Species	Analytical Method	LOD, µg/m^3	LOQ, µg/m^3	No. of Valid Values	No. > LOD	% > LOD	No. > LOQ	% > LOQ
V	XRF	0.001	0.005	360	224	62%	60	17%
Cr	XRF	0.019	0.062	360	0	0%	0	0%
Mn	XRF	0.013	0.042	360	84	23%	0	0%
Fe	XRF	0.076	0.254	360	302	84%	91	25%
Co	XRF	0.003	0.011	360	0	0%	0	0%
Ni	XRF	0.003	0.011	360	110	31%	16	4%
Cu	XRF	0.009	0.030	360	118	33%	0	0%
Zn	XRF	0.005	0.017	360	346	96%	280	78%
Ga	XRF	0.020	0.067	360	0	0%	0	0%
Ge	XRF	0.124	0.412	360	0	0%	0	0%
As	XRF	0.064	0.212	360	0	0%	0	0%
Se	XRF	0.064	0.212	360	0	0%	0	0%
Br	XRF	0.064	0.212	360	0	0%	0	0%
Rb	XRF	0.003	0.011	360	0	0%	0	0%
Sr	XRF	0.005	0.016	360	15	4%	6	2%
Y	XRF	0.004	0.015	360	0	0%	0	0%
Zr	XRF	0.012	0.038	360	0	0%	0	0%
Nb	XRF	0.010	0.032	360	0	0%	0	0%
Mo	XRF	0.007	0.024	360	0	0%	0	0%
Rh	XRF	0.013	0.042	360	1	0%	0	0%
Pd	XRF	0.014	0.046	360	0	0%	0	0%
Ag	XRF	0.012	0.040	360	0	0%	0	0%
Cd	XRF	0.012	0.040	360	0	0%	0	0%
In	XRF	0.015	0.050	360	0	0%	0	0%
Sn	XRF	0.024	0.079	360	2	1%	0	0%
Sb	XRF	0.019	0.065	360	0	0%	0	0%
Te	XRF	0.032	0.108	360	0	0%	0	0%
I	XRF	0.036	0.122	360	0	0%	0	0%
Cs	XRF	0.071	0.237	360	0	0%	0	0%
Ba	XRF	0.098	0.328	360	0	0%	0	0%
La	XRF	0.102	0.341	360	0	0%	0	0%
Ce	XRF	0.004	0.015	360	0	0%	0	0%
Sm	XRF	0.008	0.026	360	0	0%	0	0%
Eu	XRF	0.020	0.066	360	0	0%	0	0%
Tb	XRF	0.007	0.025	360	0	0%	0	0%

Species	Analytical Method	LOD, µg/m³	LOQ, µg/m³	No. of Valid Values	No. > LOD	% > LOD	No. > LOQ	% > LOQ
Hf	XRF	0.035	0.117	360	0	0%	0	0%
Ta	XRF	0.182	0.608	360	0	0%	0	0%
W	XRF	0.027	0.089	360	20	6%	0	0%
Ir	XRF	0.015	0.052	360	0	0%	0	0%
Au	XRF	0.015	0.052	360	0	0%	0	0%
Hg	XRF	0.015	0.052	360	3	1%	0	0%
Tl	XRF	0.015	0.052	360	0	0%	0	0%
Pb	XRF	0.004	0.014	360	200	56%	49	14%
U	XRF	0.015	0.050	360	0	0%	0	0%

The number of reported concentrations for each species and number of reported concentrations greater than the LODs and LOQs are also summarized in Table 7. For the 365 valid quartz fiber filter samples and 360 valid Teflon filter samples, major ions (including sulfate, nitrate, ammonium, water soluble potassium and water-soluble sodium), organic carbon, elemental carbon, sodium (Na), sulfur (S), potassium (K), calcium (Ca), and zinc (Zn) were detected (>LOD) in almost all the samples (more than 90%). A number of transition metals (e.g. Cr, Co, Zr, Nb, Rh, Pd, Ag, Cd, Hf, Ta, W, Ir, Au and Hg) were not detected in most of the samples (less than 15%). V and Ni, which are residual-oil-related species, were detected in 62% and 31% of the samples, respectively. Toxic species emitted from industrial sources, such as Cd and Hg, were almost not detected (0% and 1% of the samples, respectively). Soil/dust-related species, including Al, Si, Ca, Ti, and Fe, were found above the LODs in more than 76% of the samples and above the LOQs in more than 13% of the samples.

In general, the analytical specifications shown in Table 7 suggest that the $PM_{2.5}$ samples collected during the study period possess adequate loadings for chemical analysis. The detection limits of the selected analytical methods were sufficiently low to establish valid measurements with acceptable precision.

3.3 Data Validation

Three levels of data validation were conducted to the data set acquired from the study.

Level I data validation: 1) flag measurements for deviations from procedures; 2) identify and remove invalid values and indicate the reasons for invalid sampling, and 3) estimate precisions from replicate and blank analyses.

Level II data validation examines internal consistency tests among different data and attempts to resolve discrepancies based on known physical relationships between variables: 1) compare a sum of chemical species to mass concentrations; 2) compare measurements from different methods; 3) compare collocated measurements; 4) examine time series from different sites to identify and investigate outliers, and 5) prepare a data qualification statement.

Level III data validation is part of the data interpretation process and should identify unusual values including: 1) extreme values; 2) values which would otherwise normally track the values of other variables in a time series, and 3) values for observables which would normally follow a qualitatively predictable spatial or temporal pattern. External consistency tests are used to identify values in the data set which appear atypical when compared to other data sets. The first assumption upon finding a measurement which is inconsistent with physical expectations is that the unusual value is due to a measurement error. If nothing unusual is found upon tracing the path of the measurement, the value would be assumed to be a valid result of an environmental cause.

Level I data validation was performed and the validation flags and comments are stated in the database as documented in Section 3.1. Level II validation tests and results are described in the following subsections including 1) sum of chemical species versus $PM_{2.5}$ mass; 2) physical and chemical consistency; 3) anion/cation balance; 4) carbon measurements by different thermal/optical methods; 5) reconstructed versus measured mass, and 6) collocated measurement comparison. For Level III data validation, parallel consistency tests were applied to data sets from the same population (e.g., region, period of time) by different data analysis approaches. Collocated samples collected at two out of the five sampling sites were examined. Comparison of $PM_{2.5}$ mass concentrations obtained from gravimetric analysis and from 24-hr average continuous measurements were also conducted. The Level III data validation continues for as long as the database is maintained. For Level II/III data validation in this study, correlations and linear regression statistics were performed on the valid data set and scatter plots were generated for better comparison.

3.3.1 Sum of Chemical Species versus $PM_{2.5}$ Mass

The sum of the individual chemical concentrations determined in this study for $PM_{2.5}$ samples should be less than or equal to the corresponding mass concentrations obtained from gravimetric measurements. The chemical species include those that were quantified on both Teflon-membrane filters and quartz fiber filters. To avoid double counting, chloride (Cl^-), total potassium (K), soluble sodium (Na^+), and sulfate (SO_4^{2-}) are included in the sum while total sulfur (S), total chlorine (Cl), total sodium (Na), and soluble potassium (K^+) are excluded. Carbon concentration is represented by the sum of organic carbon and elemental carbon. Unmeasured ions, metal oxides, or hydrogen and oxygen associated with organic carbon are not counted into the measured concentrations.

The sum of chemical species was plotted against the measured $PM_{2.5}$ mass on Teflon filters for each of the individual sites in Figure 2. Linear regression analysis results and the average ratios of Y over X are both shown in Table 8 for comparison. Each plot contains a solid line indicating the slope with intercept and a dashed 1:1 line. Measurement uncertainties associated with the x- and y-axes are shown and the uncertainties of the $PM_{2.5}$ mass data were assumed to be 5% of the concentrations.

A strong correlation (R^2 = 0.98) was found between the sum of measured species and mass with a slope of 0.788±0.007 (Figure 2f).

Limits used for identifying reconstructed mass outliers refer to those in Speciation Trends Network program suggested by USEPA [2012] and are listed as follows,

Lower Limit: [Sum of Chemical Species]/[Measured Mass] = 0.60

Upper Limit: [Sum of Chemical Species]/[Measured Mass] = 1.32

Based on these criteria, one sample is flagged as an outlier. This sample is WB220710, with an X/Y ratio of 0.59. The $PM_{2.5}$ concentration of this sample is 3.87 μg/m^3, which is among the lowest values of the collected samples. It is noted that this test is helpful for sites with appreciable filter loadings and has been found less useful for lower level filter loading [RTI, 2005].

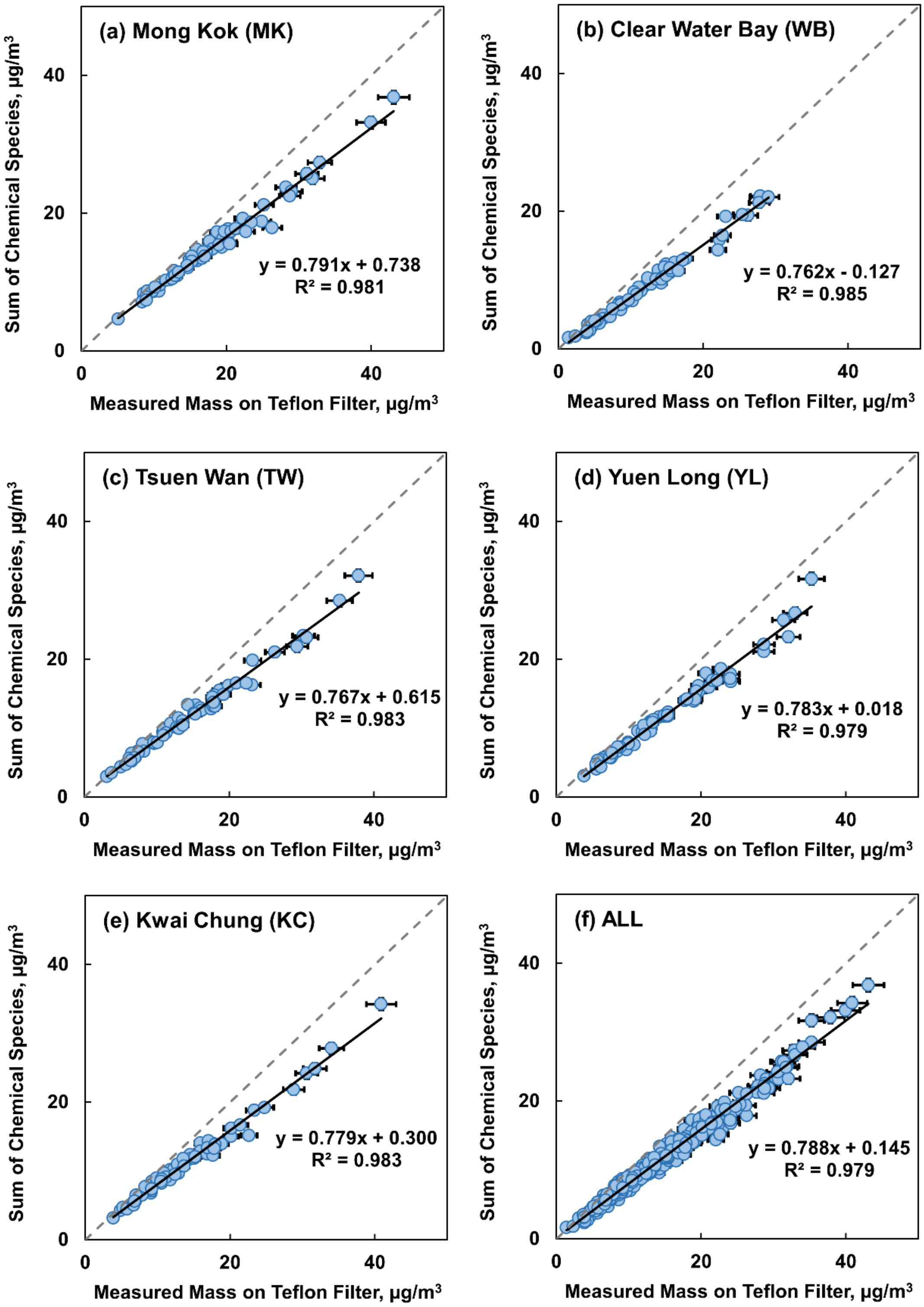

Figure 2. Scatter plots of sum of measured chemical species versus measured mass on Teflon filter for PM2.5 samples collected at (a) MK, (b) WB, (c) TW, (d) YL, (e) KC, and (f) all sites.

Table 8. Statistics analysis of sum of measured chemical species versus measured mass on Teflon filters for $PM_{2.5}$ samples collected in this study (Quotation Ref. 21-02409)

Statistics/Site	MK	WB	TW	YL	KC	ALL
n	60	61	57	61	61	300
Slope	0.791 (±0.015)	0.762 (±0.012)	0.767 (±0.014)	0.783 (±0.015)	0.779 (±0.013)	0.788 (±0.007)
Intercept	0.738 (±0.283)	-0.127 (±0.178)	0.615 (±0.225)	0.018 (±0.253)	0.300 (±0.218)	0.145 (±0.114)
R^2	0.981	0.985	0.983	0.979	0.983	0.979
AVG sum	14.81	9.49	11.86	11.80	11.73	11.93
AVG mass	17.80	12.61	14.67	15.04	14.67	14.95
AVG sum/mass	0.842 (±0.05)	0.754 (±0.078)	0.825 (±0.061)	0.788 (±0.052)	0.808 (±0.054)	0.803 (±0.067)

3.3.2 Physical and Chemical Consistency

Measurements of chemical species concentrations conducted by different methods are compared. Physical and chemical consistency tests include: 1) sulfate (SO_4^{2-}) versus total sulfur (S), 2) soluble potassium (K^+) versus total potassium (K), 3) chloride (Cl^-) versus chlorine (Cl), and 4) ammonium balance.

3.3.2.1 Water-Soluble Sulfate (SO_4^{2-}) versus Total Sulfur (S)

SO_4^{2-} is measured by IC on quartz fiber filters and total S is measured by ED-XRF on Teflon filters. The theoretical ratio of SO_4^{2-} to S is approximately 3, based on their molecular weights and assuming all of the sulfur is present as SO_4^{2-}. Since SO_4^{2-} and total S are collected on different filters, this ratio is helpful for diagnosing flow rate problems of the samplers.

Figure 3 shows the scatter plots of SO_4^{2-} versus total S concentrations for each of the five sites. A good correlation (R^2 = 0.98) was observed for the aggregated data from all the sites, with a slope of 2.407±0.021 and an intercept of -0.076±0.037. The average sulfate to total sulfur ratio is determined to be 2.295±0.240, which meets the validation criteria (SO_4^{2-}/total S < 3.0).

Good correlations (R^2 = 0.97–0.98) were found for sulfate/total sulfur in $PM_{2.5}$ samples collected at individual sites. The regression statistics suggest a slope ranging from 2.345±0.056 to 2.436±0.049 and the intercepts are all at relatively low levels. The average sulfate/sulfur ratio ranges from 2.270±0.252 to 2.330±0.225 (Table 9). Both of the calculations indicate that the majority of the sulfur was present as soluble sulfate in $PM_{2.5}$.

Limits for outliers as suggested by USEPA [2012] are as follows,

Lower Limit: $[S]/[SO_4^{2-}] = 0.25$

Upper Limit: $[S]/[SO_4^{2-}] = 0.45$

94 samples are flagged as outliers (all above the upper limit) and the top ten outliers above the upper limit are listed in Table 10 with the corresponding mass, SO_4^{2-}, S concentrations and the $[S]/[SO_4^{2-}]$ ratios. Since the chemical information was obtained from two types of filter substrates, the % differences of masses obtained from Teflon filters and quartz fiber filters (column "T vs. Q %Diff") were also included for ease of reference. The main causes of the outliers may include: 1) larger sampling and measurement uncertainties due to the very low particle loading (2 samples, as highlighted in light blue, are with $PM_{2.5}$ mass concentrations below 10 $\mu g/m^3$) and 2) various sulfur existing in forms other than sulfate.

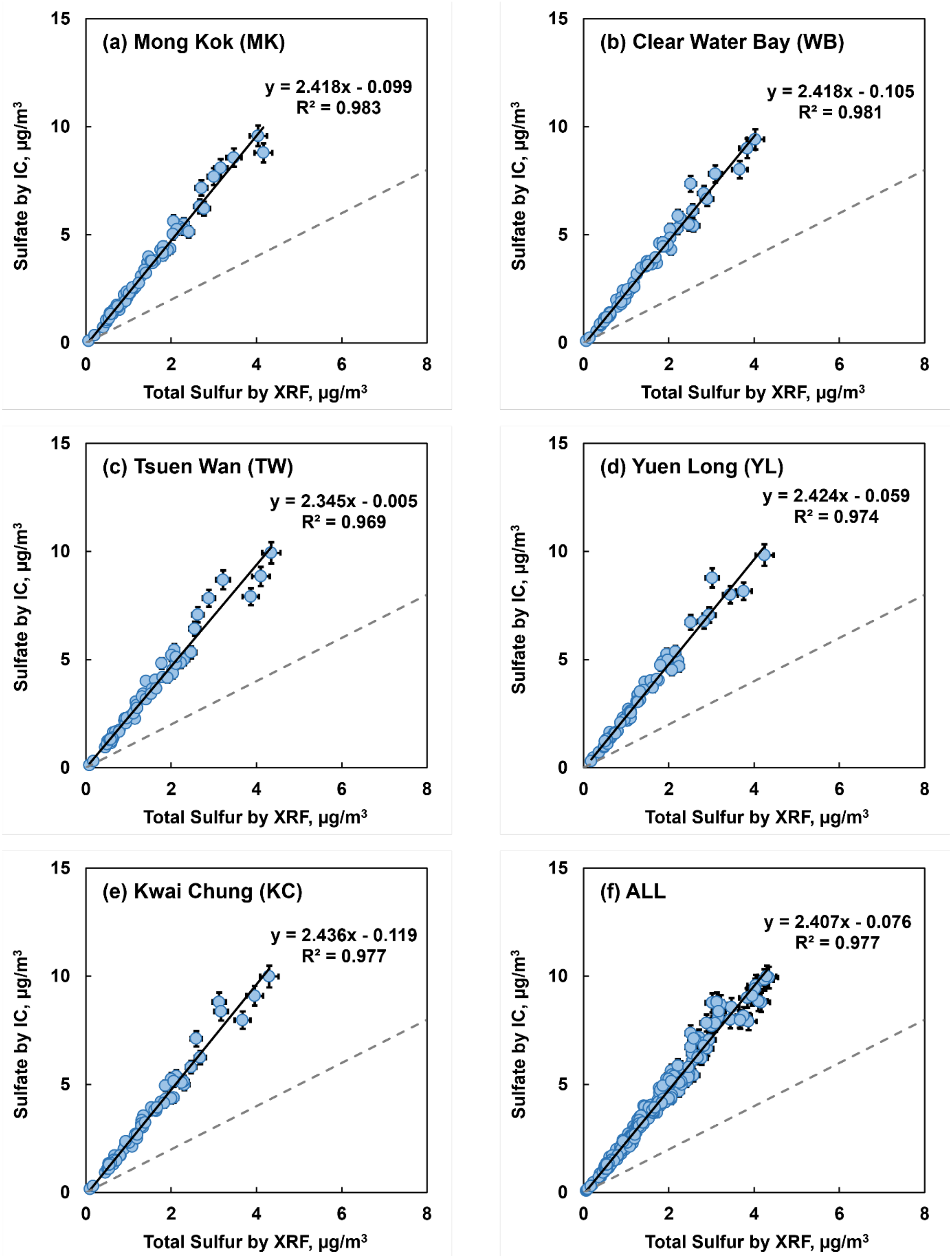

Figure 3. Scatter plots of sulfate versus total sulfur measurements for $PM_{2.5}$ samples collected at (a) MK, (b) WB, (c) TW, (d) YL, (e) KC, and (f) all sites.

Table 9. Statistics analysis of sulfate versus total sulfur measurements for $PM_{2.5}$ samples collected in this study (Quotation Ref. 21-02409)

Statistics/Site	MK	WB	TW	YL	KC	ALL
n	60	61	57	61	61	300
Slope	2.418 (±0.041)	2.418 (±0.044)	2.345 (±0.056)	2.424 (±0.051)	2.436 (±0.049)	2.407 (±0.021)
Intercept	-0.099 (±0.072)	-0.105 (±0.075)	-0.005 (±0.099)	-0.059 (±0.085)	-0.119 (±0.085)	-0.076 (±0.037)
R^2	0.983	0.981	0.969	0.974	0.977	0.977
AVG SO_4^{2-}	3.50	3.44	3.50	3.38	3.51	3.47
AVG total S	1.49	1.46	1.5	1.42	1.49	1.47
AVG SO_4^{2-}/S	2.283 (±0.241)	2.27 (±0.252)	2.294 (±0.252)	2.330 (±0.234)	2.300 (±0.225)	2.295 (±0.24)

Table 10. List of the ten examples of flagged samples from the [S]/[SO_4^{2-}] test with ratio > 0.45

Sample ID	$PM_{2.5}$ mass conc. from Teflon Sample (µg/m^3)	$PM_{2.5}$ mass conc. from Quartz Sample (µg/m^3)	T vs. Q %Diff	SO_4^{2-} conc. (µg/m^3)	S conc. (µg/m^3)	[S]/[SO_4^{2-}] Ratio
MK220222	5.08	5.42	6%	0.082	0.066	0.801
WB220222	1.41	2.79	65%	0.085	0.064	0.751
TW220222	3.12	4.17	29%	0.118	0.086	0.723
KC220222	4.86	6.82	33%	0.157	0.097	0.617
WB220809	2.37	4.82	68%	0.238	0.146	0.612
YL220809	3.83	5.70	39%	0.298	0.181	0.606
TW220809	3.78	5.62	39%	0.300	0.181	0.601
KC220809	3.87	6.40	49%	0.289	0.171	0.592
MK220809	8.42	11.79	33%	0.347	0.202	0.582
MK220610	10.71	11.96	11%	0.716	0.408	0.570

3.3.2.2 Water-soluble Potassium (K^+) versus Total Potassium (K)

K^+ is measured by IC on quartz fiber filters and the total K is measured by ED-XRF on Teflon filters. The ratio of K^+ to K is expected to be equal to or less than 1. Figure 4 shows the scatter plots of K^+ versus total K concentrations for each of the five sites. A good correlation (R^2 = 0.97) was observed for all the sites with a slope of 0.790±0.008 and an intercept of -0.017±0.002. The ratio of water-soluble potassium to total potassium averages at 0.649±0.213, which meets the validation criteria (K^+/total K < 1).

Good correlations (R^2 = 0.96–0.98) were found for K^+/K in $PM_{2.5}$ samples collected at individual sites. The regression statistics show that the slope ranges from 0.771±0.017 to 0.809±0.023 and the intercepts are all at relatively low levels (Table 11). Generally, most of the total potassium is in its soluble ionic form.

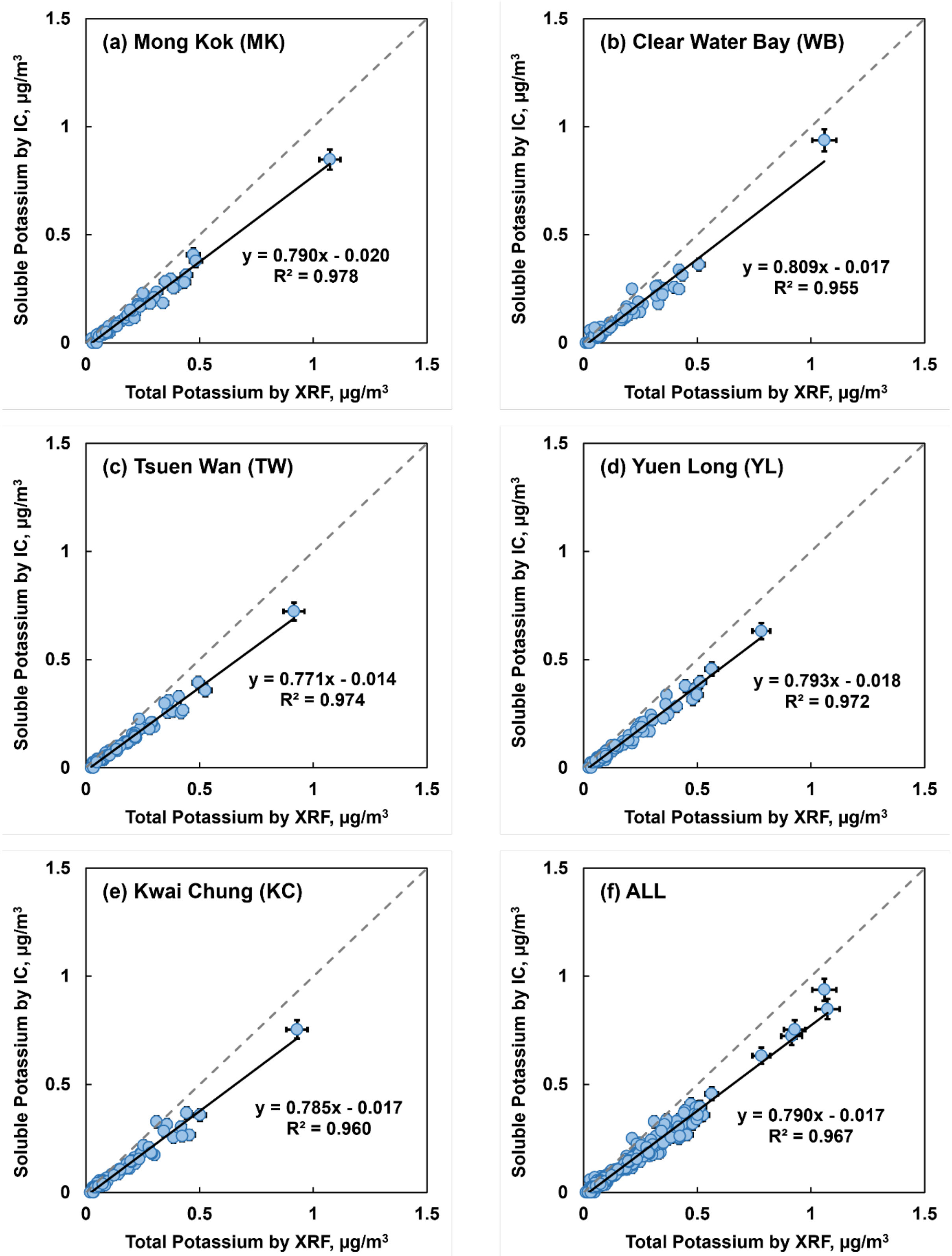

Figure 4. Scatter plots of water-soluble potassium versus total potassium measurements for $PM_{2.5}$ samples collected at (a) MK, (b) WB, (c) TW, (d) YL, (e) KC, and (f) all sites.

Table 11. Statistics analysis of water-soluble potassium versus total potassium measurements for $PM_{2.5}$ samples collected in this study (Quotation Ref. 21-02409)

Statistics/Site	MK	WB	TW	YL	KC	ALL
n	60	61	57	61	61	300
Slope	0.790 (±0.016)	0.809 (±0.023)	0.771 (±0.017)	0.793 (±0.017)	0.785 (±0.021)	0.790 (±0.008)
Intercept	-0.020 (±0.004)	-0.017 (±0.006)	-0.014 (±0.004)	-0.018 (±0.005)	-0.017 (±0.005)	-0.017 (±0.002)
R^2	0.978	0.955	0.974	0.972	0.96	0.967
AVG total K	0.14	0.13	0.14	0.15	0.13	0.14
AVG K^+	0.20	0.18	0.20	0.21	0.19	0.20
AVG K^+/K	0.633 (±0.176)	0.670 (±0.317)	0.647 (±0.18)	0.657 (±0.165)	0.636 (±0.193)	0.649 (±0.213)

3.3.2.3 Chloride (Cl^-) versus Chlorine (Cl)

Cl^- is measured by IC on quartz fiber filters and the total chlorine (Cl) is measured by ED-XRF on Teflon filters. The ratio of Cl^- to Cl is expected to equal or be less than 1. Figure 5 shows the scatter plots of Cl^- versus total Cl concentrations for each of the five sites. Moderate correlations ($R^2 = 0.815$) were found for the combined data of all the sampling sites. The slope values (0.578–0.876) deviate, to a notable degree, from unity. The uncertainties of Cl^-/Cl measurements are mainly associated with the volatility of Cl. On one hand, a portion of Cl^- could be lost during the storage of the quartz fiber filters especially when the aerosol samples are acidic. On the other hand, some Cl would be volatized in the vacuum chamber during the ED-XRF analysis. Such losses are more significant when Cl concentrations are low.

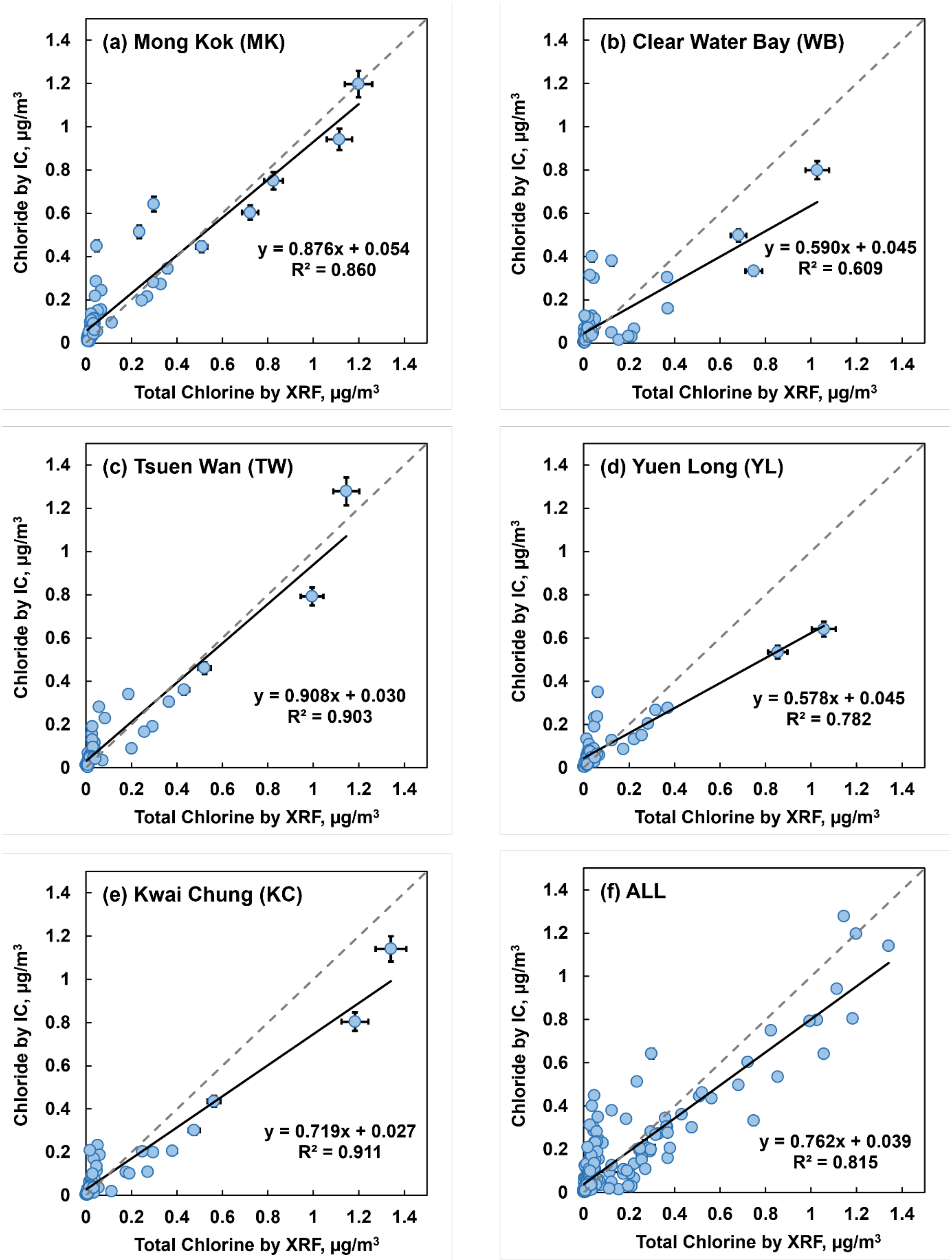

Figure 5. Scatter plots of chloride versus total chlorine measurements for $PM_{2.5}$ samples collected at (a) MK, (b) WB, (c) TW, (d) YL, (e) KC, and (f) all sites.

Table 12. Statistics analysis of chloride versus total chlorine measurements for $PM_{2.5}$ samples collected in this study (Quotation Ref. 21-02409)

Statistics/Site	MK	WB	TW	YL	KC	ALL
n	60	61	57	61	61	300
Slope	0.876 (±0.046)	0.590 (±0.061)	0.908 (±0.04)	0.578 (±0.04)	0.719 (±0.029)	0.762 (±0.021)
Intercept	0.054 (±0.013)	0.045 (±0.013)	0.030 (±0.009)	0.045 (±0.008)	0.027 (±0.008)	0.039 (±0.005)
R^2	0.860	0.609	0.903	0.782	0.911	0.815
AVG Cl^-	0.17	0.09	0.12	0.09	0.10	0.11
AVG total Cl	0.13	0.08	0.10	0.08	0.10	0.10
AVG Cl^-/Cl	2.323 (±1.636)	3.470 (±4.192)	2.385 (±1.507)	2.314 (±1.613)	2.105 (±1.705)	2.521 (±2.411)

3.3.2.4 Ammonium Balance

To further validate the ion measurements, calculated versus measured ammonium (NH_4^+) are compared. NH_4^+ is directly measured by IC analysis of quartz fiber filter extract. NH_4^+ in atmospheric aerosols is found in the chemical forms of NH_4NO_3, $(NH_4)_2SO_4$, and NH_4HSO_4 while NH_4Cl is usually negligible and excluded from the calculation. Assuming full neutralization, measured NH_4^+ can be compared with the computed NH_4^+, which can be calculated in the following two ways corresponding to assuming the association of NH_4^+ with sulfate to be $(NH_4)_2SO_4$ and NH_4HSO_4, respectively:

Calculated NH_4^+ based on NH_4NO_3 and $(NH_4)_2SO_4$ = $0.29 \times [NO_3^-] + 0.374 \times [SO_4^{2-}]$

Calculated NH_4^+ based on NH_4NO_3 and NH_4HSO_4 = $0.29 \times [NO_3^-] + 0.187 \times [SO_4^{2-}]$

The calculated NH_4^+ is plotted against measured NH_4^+ for each of the five sites in Figure 6. For both forms of sulfate the comparisons show strong correlations ($R^2 > 0.9$) but with different slopes. The slopes for individual sampling sites range from 1.038±0.033 at WB to 1.063±0.028 at MK assuming ammonium sulfate, and from 0.592±0.026 at WB to 0.686±0.029 at MK assuming ammonium bisulfate. These values are close to those found in earlier years. The average ratios of calculated ammonium to measured ammonium (see Table 13) suggest that ammonium sulfate is the dominant form for sulfate in the $PM_{2.5}$ over the Hong Kong region in the year of 2022.

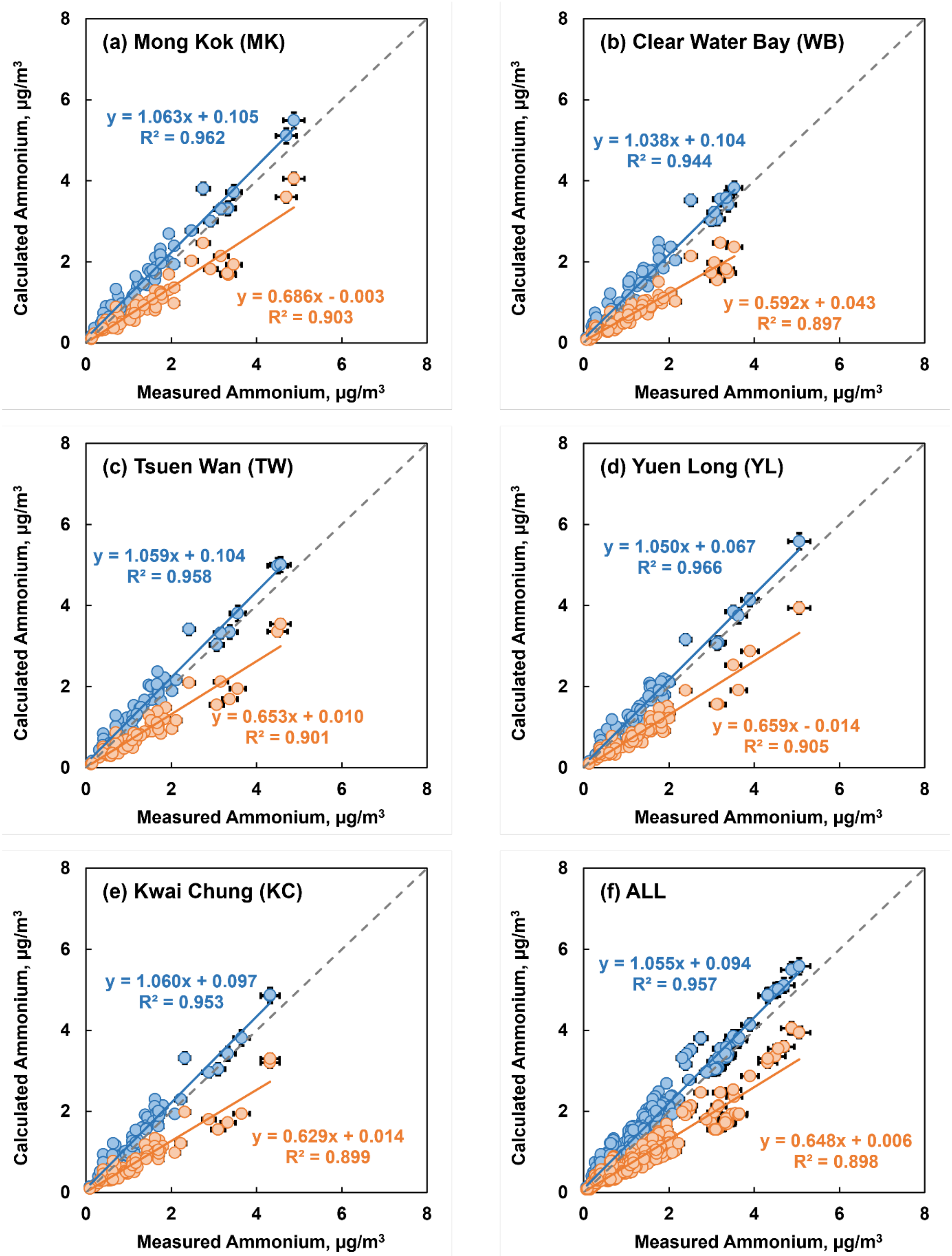

Figure 6. Scatter plots of calculated ammonium versus measured ammonium for $PM_{2.5}$ samples collected at (a) MK, (b) WB, (c) TW, (d) YL, (e) KC, and (f) all sites. The calculated ammonium data are obtained assuming all nitrate was in the form of ammonium nitrate and all sulfate was in the form of either ammonium sulfate (data in blue) or ammonium bisulfate (data in orange).

Table 13. Statistics analysis of calculated ammonium versus measured ammonium for $PM_{2.5}$ samples collected in this study (Quotation Ref. 21-02409)

Statistics/Site	MK	WB	TW	YL	KC	ALL
n	60	61	57	61	61	300
Ammonium Sulfate (blue dots)						
Slope	1.063 (±0.028)	1.038 (±0.033)	1.059 (±0.03)	1.050 (±0.026)	1.060 (±0.031)	1.055 (±0.013)
Intercept	0.105 (±0.049)	0.104 (±0.052)	0.104 (±0.051)	0.067 (±0.044)	0.097 (±0.05)	0.094 (±0.022)
R^2	0.962	0.944	0.958	0.966	0.953	0.957
AVG Cal. NH_4^+	1.64	1.46	1.57	1.55	1.51	1.54
AVG Mea. NH_4^+	1.45	1.30	1.38	1.41	1.33	1.37
AVG Cal./Mea. NH_4^+	1.186 (±0.236)	1.197 (±0.366)	1.168 (±0.237)	1.131 (±0.224)	1.182 (±0.272)	1.173 (±0.272)
Ammonium Bisulfate (orange dots)						
Slope	0.686 (±0.029)	0.592 (±0.026)	0.653 (±0.029)	0.659 (±0.028)	0.629 (±0.028)	0.648 (±0.013)
Intercept	-0.003 (±0.052)	0.043 (±0.041)	0.010 (±0.049)	-0.014 (±0.047)	0.014 (±0.045)	0.006 (±0.021)
R^2	0.903	0.897	0.901	0.905	0.899	0.898
AVG Cal. NH_4^+	0.99	0.81	0.91	0.92	0.85	0.90
AVG Mea. NH_4^+	1.45	1.30	1.38	1.41	1.33	1.37
AVG Cal./Mea. NH_4^+	0.716 (±0.176)	0.673 (±0.222)	0.684 (±0.173)	0.670 (±0.161)	0.673 (±0.186)	0.683 (±0.185)

3.3.3 Charge Balance

For the anion and cation balance, the sum of Cl^-, NO_3^-, and SO_4^{2-} is compared to the sum of NH_4^+, Na^+, and K^+ in μeq/m³ using the following equations:

$$\mu eq/m^3\ for\ anions\ = \left(\frac{Cl^-}{35.453} + \frac{NO_3^-}{62.005} + \frac{SO_4^{2-}}{96/2}\right)$$

$$\mu eq/m^3\ for\ cations\ = \left(\frac{NH_4^+}{18.04} + \frac{Na^+}{23.0} + \frac{K^+}{39.098}\right)$$

The anion equivalents are plotted against the cation equivalents in Figure 7. A strong correlation ($R^2 = 0.99$) is observed for the $PM_{2.5}$ samples collected at all of the sampling sites. Seen from Figure 7, the slopes obtained from individual sites range from 1.031±0.015 to 1.057±0.015 while the average Σanion/Σcation ratios range from 0.917±0.073 to 0.949±0.068 (Table 14).

The limits used for identifying outliers suggested by USEPA [2012] are as follows,

Lower Limit: [Sum of Anions]/[Sum of Cations] = 0.86

Upper Limit: [Sum of Anions]/[Sum of Cations] = 2.82

Based on these criteria, 50 samples were identified as outliers in this dataset (all below the lower limit), and the top ten outliers below the lower limit are listed in Table 15 with the corresponding mass concentrations and the Σanion/Σcation ratios. The main cause of the outliers is the larger sampling and measurement uncertainties due to the very low particle loading. 44 out of the 50 samples are with $PM_{2.5}$ mass concentrations below 10 μg/m³ (based on Teflon mass), as highlighted in light blue in Table 15.

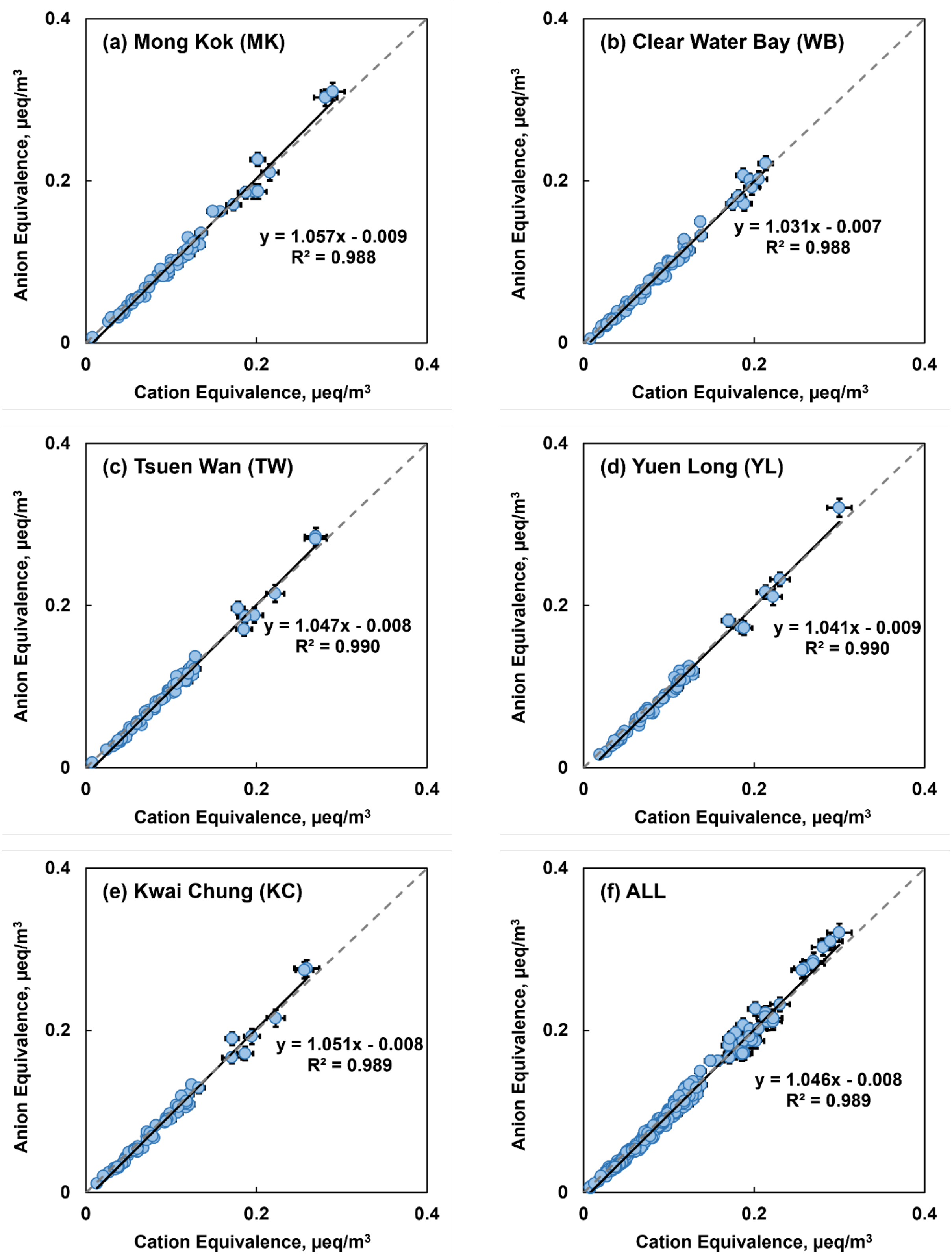

Figure 7. Scatter plots of anion versus cation measurements for $PM_{2.5}$ samples collected at (a) MK, (b) WB, (c) TW, (d) YL, (e) KC, and (f) all sites.

Table 14. Statistics analysis of anion versus cation measurements for $PM_{2.5}$ samples collected in this study (Quotation Ref. 21-02409)

Statistics/Site	MK	WB	TW	YL	KC	ALL
n	60	61	57	61	61	300
Slope	1.057 (±0.015)	1.031 (±0.015)	1.047 (±0.014)	1.041 (±0.014)	1.051 (±0.015)	1.046 (±0.006)
Intercept	-0.009 (±0.002)	-0.007 (±0.001)	-0.008 (±0.002)	-0.009 (±0.001)	-0.008 (±0.002)	-0.008 (±0.001)
R^2	0.988	0.988	0.990	0.990	0.989	0.989
AVG ∑anion	0.10	0.08	0.09	0.09	0.09	0.09
AVG ∑cation	0.10	0.09	0.09	0.09	0.09	0.09
AVG ∑anion/∑cation	0.949 (±0.068)	0.921 (±0.088)	0.928 (±0.074)	0.917 (±0.073)	0.933 (±0.072)	0.929 (±0.076)

Table 15. List of flagged samples from the charge balance test

Sample ID	$PM_{2.5}$ mass conc. from Teflon Sample ($\mu g/m^3$)	$PM_{2.5}$ mass conc. from Quartz Sample ($\mu g/m^3$)	$\sum$anion eqv., ($\mu eq/m^3$)	$\sum$cation eqv., ($\mu eq/m^3$)	$\sum$anion/$\sum$cation Ratio
WB220222	1.41	2.79	0.005	0.008	0.623
YL220610	5.54	6.61	0.020	0.027	0.732
WB220610	4.57	7.90	0.013	0.018	0.754
WB220616	4.53	5.03	0.021	0.027	0.769
WB220815	5.32	8.65	0.030	0.038	0.779
TW220628	6.54	9.25	0.037	0.047	0.782
YL220628	5.71	8.29	0.035	0.044	0.784
YL220710	5.50	7.82	0.030	0.038	0.785
TW220710	5.74	8.33	0.032	0.040	0.786
WB220803	8.69	10.85	0.039	0.050	0.786

3.3.4 Carbon Measurements

3.3.4.1 TOT versus TOR

Carbon concentrations were determined for the collected $PM_{2.5}$ samples by both TOR and TOT methods. The comparison results of OC and EC determined by both methods for individual sites are shown in Figures 8 and 9, respectively. Generally, EC concentrations derived by the TOT method were much lower than those by the TOR method. The difference in EC obtained by these two methods has been well-documented and is primarily a result of method-dependent nature of correction of charring of OC formed during thermal analysis [e.g., Chow et al.,2004; Chen et al., 2004]. Seen from the results, the average ratios of TOT EC to TOR EC for samples from individual sampling sites range from 0.862±0.131 at WB to 0.916±0.064 at MK (Table 16).

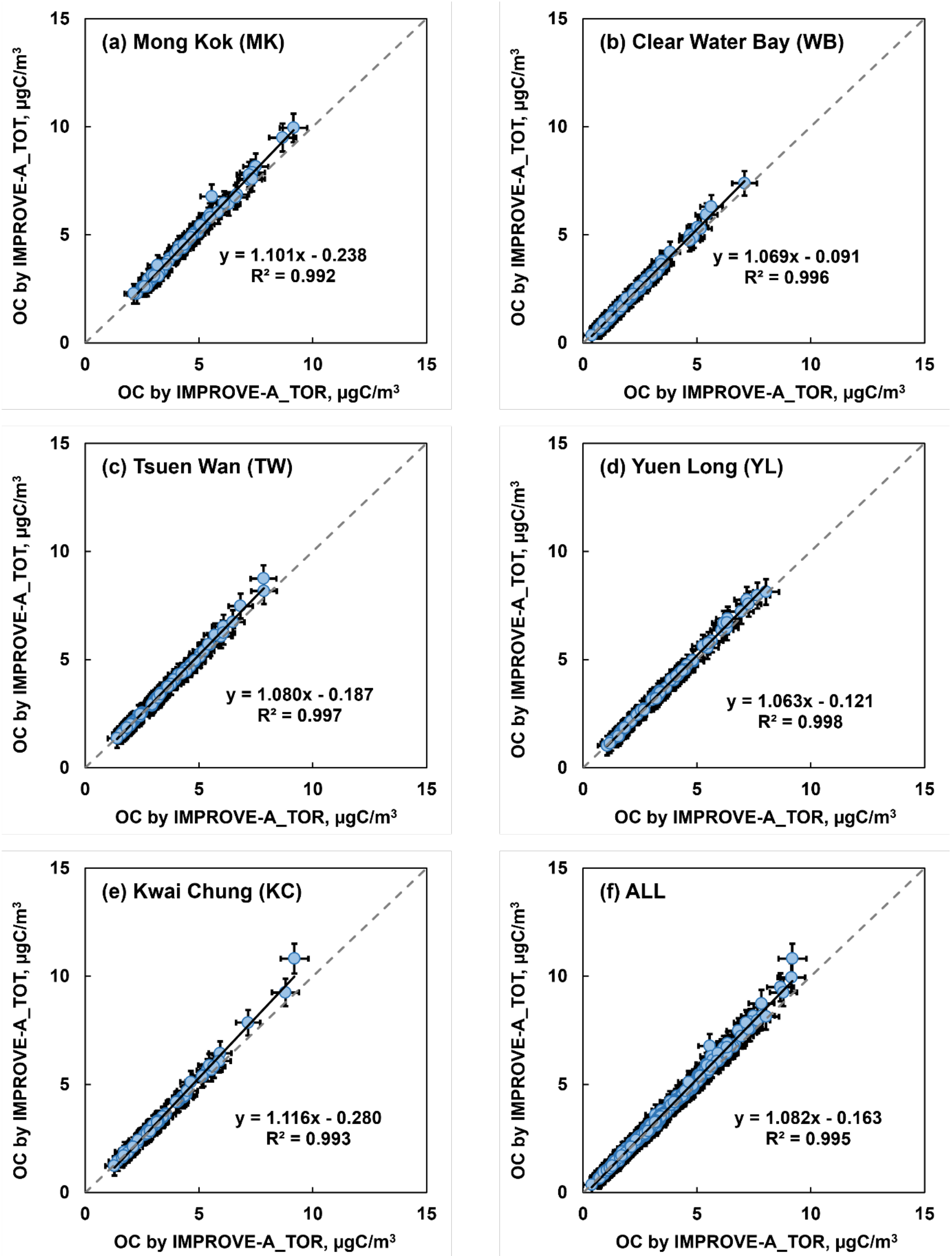

Figure 8. Comparisons of OC determined by TOR and TOT methods for $PM_{2.5}$ samples collected at (a) MK, (b) WB, (c) TW, (d) YL, (e) KC, and (f) all sites.

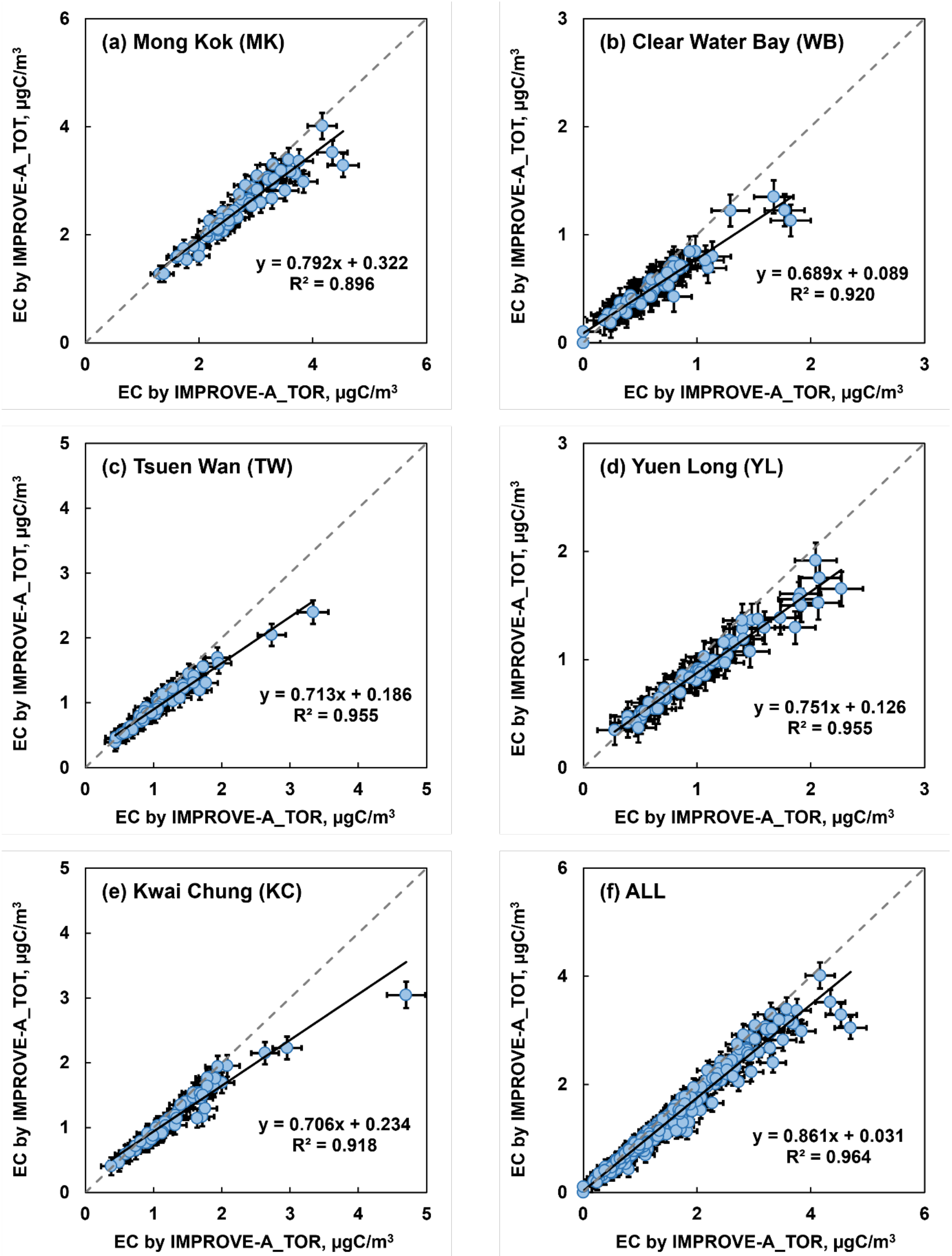

Figure 9. Comparisons of EC determined by TOR and TOT methods for $PM_{2.5}$ samples collected at (a) MK, (b) WB, (c) TW, (d) YL, (e) KC, and (f) all sites.

Table 16. Statistics analysis of OC and EC determined by TOR and TOT methods for $PM_{2.5}$ samples collected in this study (Quotation Ref. 21-02409)

Statistics/Site	MK	WB	TW	YL	KC	ALL
n	60	61	57	61	61	300
TOT OC versus TOR OC						
Slope	1.101 (±0.013)	1.069 (±0.008)	1.080 (±0.008)	1.063 (±0.006)	1.116 (±0.012)	1.082 (±0.004)
Intercept	-0.238 (±0.064)	-0.091 (±0.024)	-0.187 (±0.034)	-0.121 (±0.025)	-0.280 (±0.047)	-0.163 (±0.017)
R^2	0.992	0.996	0.997	0.998	0.993	0.995
AVG TOT_OC	4.69	2.56	3.83	3.83	3.75	3.73
AVG TOR_OC	4.48	2.48	3.72	3.72	3.61	3.60
AVG TOT_OC/TOR_OC	1.041 (±0.041)	1.015 (±0.046)	1.021 (±0.027)	1.020 (±0.031)	1.029 (±0.033)	1.025 (±0.038)
TOT EC versus TOR EC						
Slope	0.792 (±0.035)	0.689 (±0.027)	0.713 (±0.021)	0.751 (±0.021)	0.706 (±0.027)	0.861 (±0.01)
Intercept	0.322 (±0.1)	0.089 (±0.02)	0.186 (±0.026)	0.126 (±0.025)	0.234 (±0.042)	0.031 (±0.016)
R^2	0.896	0.920	0.955	0.955	0.918	0.964
AVG TOT_EC	2.49	0.53	1.00	0.94	1.21	1.23
AVG TOR_EC	2.73	0.64	1.15	1.08	1.38	1.39
AVG TOT_EC/TOR_EC	0.916 (±0.064)	0.862 (±0.131)	0.896 (±0.074)	0.895 (±0.1)	0.894 (±0.08)	0.893 (±0.094)

3.3.4.2 OC artifacts

Three pieces of 47-mm quartz filters (Filter A, B and C) pre-baked at 900°C on 13 December 2022 were subjected to OCEC analysis on a weekly basis. Except during OCEC analysis, the filters were kept in the chamber used for filter conditioning, with chamber door slightly opened. The chamber is located in the temperature and RH controlled balance room. Inside the chamber, the filters were kept in petri dishes with lid being ¼ opened. All these procedures are practiced in the routine filter preparation for the $PM_{2.5}$ weighing project.

The first analysis was conducted on the next day (14 December) after the filters were baked, which is denoted as Week 0. The results of Filter A and B are consistent while that of Filter C is questionable and hence only A and B are considered. Figure 10 below shows the carbon mass (in µgC/filter punch of 0.522 cm^2) determined from Week 0 to Week 6 for TC and the subfractions including OC, EC, and OC1 to OC4.

Figure 10(a) shows TC increased with the filter conditioning time over the entire experimental period. Comparing the changes in OC and EC shown in panels (b) and (c), one can see the increase was exclusively attributed to OC, consistent with adsorption of background VOCs on the filters. Panels (d) to (g) indicate OC1 to OC3 accounted for most of the adsorbed OC. The magnitudes of increase over the six weeks were 0.12 µgC/punch for OC1, 0.18 µgC/punch for OC2 and 0.30 µgC/punch for OC3. Overall, the OC content tripled from 0.17 µgC/punch in Week 0 to 0.61 µgC/punch in Week 6. It appears that the OC had levelled off since Week 4. This time length corresponds to the amount of time required for conditioning quartz filter to obtain a stabilized weighing result.

If we assume a sampling volume of 24 m^3 and 11.98 cm^2 effective deposit area on the filter as in regular $PM_{2.5}$ samples, the 0.61 µgC/punch (or 1.2 µgC/cm^2) translates to an ambient concentration of 0.58 µgC/m^3. The average field blank concentration from the five $PM_{2.5}$ speciation sampling sites during January–December 2022 was 0.80±0.33 µgC/m^3 (±1 standard deviation). This means about 70% of the reported field blank value was associated with lab exposure during the filter conditioning processes. If we express in term of µgC/cm^2 of filter area, the lab blank is 1.2 µgC/cm^2 and the field blank is 1.6 ±0.6 µgC/cm^2.

For comparison, the European Union specifies in its standard operating procedure (SOP) for OC and EC (BS EN 16909:2017) that (1) the OC content for lab blanks shall not be above 2 µgC/cm^2 and (2) the field blanks are up to 4 µgC/cm^2 (European Committee for Standardization, 2017). The SOP adopted by the Chemical Speciation Network in the US specifies an acceptance criterion of ≤1.0 µgC/cm^2 for lab blank (Air Quality Research Center of the UC-Davis, 2022). In this speciation network, the field blank from 1678 field blanks collected in 2022 was reported to be 2.14±1.57 µgC/cm^2 (Air Quality Research Center of the UC-Davis, 2023). Thus, the lab blanks and the field blanks obtained in this project meet the European Union standard and compare favorably with those reported for the US Chemical Speciation Network.

Table 17 presents the ambient concentration of OC for the five sites averaged from January–December 2022. The 0.58 µgC/m^3 OC artifact resulting from lab exposure could amount to a percentage contribution ranging from 12.9% for MK up to 23.4% for WB. Blank correction has been made to OC concentrations to avoid such a bias.

In summary, the experiment shows that the filter conditioning process required for quartz fibre filter to produce stabilized weighing result would introduce 12.9–23.4% of positive bias to OC measurements, resulting from the uncontrollable adsorption of VOCs existing in the weighing lab background. The lower the ambient OC concentration is, the greater the influence of positive artifact will be introduced.

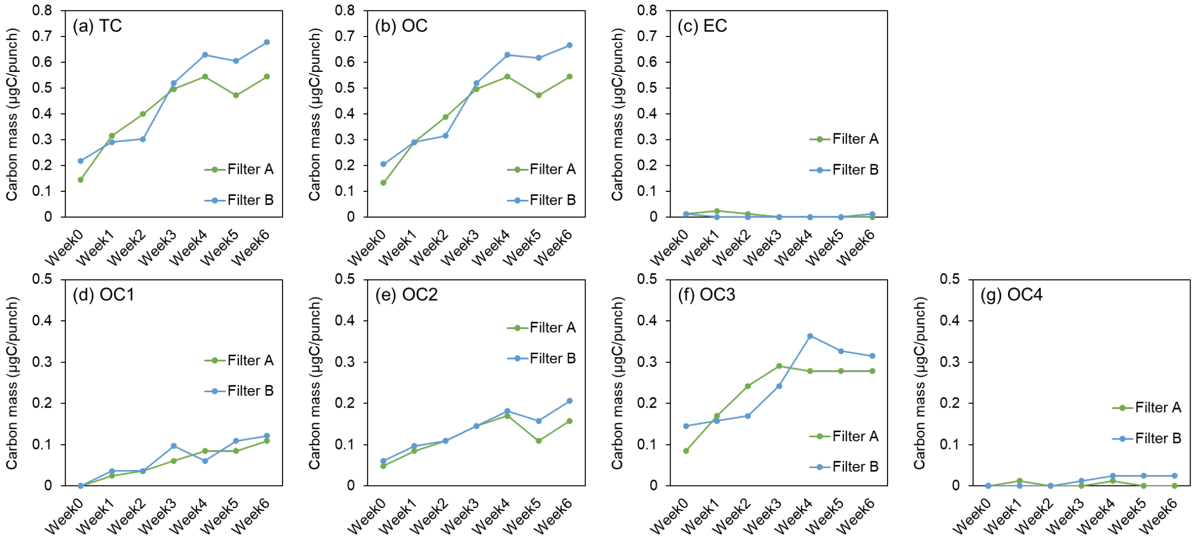

Figure 10. Carbon masses determined on Filter A and B from Week 0 to Week 6: (a) total carbon; (b) organic carbon, (c) Elemental carbon, (d) OC1, (e) OC2, (f) OC3, and (g) OC4.

Table 17. Average OC concentration during January–December 2022 and percentage contribution from OC artifact from lab exposure

	MK	WB	TW	KC	YL
OC, μgC/m^3	4.48	2.48	3.72	3.72	3.61
% OC artifact	12.9	23.4	15.6	15.6	16.1

3.3.5 Material Balance

Major PM components can be classified into the following categories: 1) geological material, which can be estimated by (1.89 × [Al] + 2.14 × [Si] + 1.4 × [Ca] + 1.43 × [Fe]); 2) organic matter (OM), which can be estimated from OC concentration as [OM] = 1.4 × [OC]; 3) soot which can be represented by EC concentration; 4) ammonium; 5) sulfate; 6) nitrate; 7) non-crustal trace elements; and 8) unidentified material. Considering the large uncertainty in Na measurement by ED-XRF, water-soluble sodium is used in calculation instead of total sodium. Therefore, the reconstructed mass is calculated by the following equation,

[Reconstructed Mass]

= 1.89 × [Al] + 2.14 × [Si] + 1.4 × [Ca] + 1.43 × [Fe]

+ 1.4 × [OC]

+ [EC]

+ $[NH_4^+]$

+ $[Na^+]$

+ [K]

+ $[SO_4^{2-}]$

+ $[NO_3^-]$

+ trace elements excluding Na, Al, Si, K, Ca, Fe, and S

The reconstructed mass is plotted against the measured mass in Figure 11. A strong correlation ($R^2 = 0.99$) is observed between the reconstructed mass and measured mass with a slope of 0.892±0.007. Different from the comparison made between sum of chemical species and measured mass (Figure 2), the major uncertainty of the reconstructed mass is due to the estimation of OM. The concentration of OM is determined by multiplying the OC concentration by an empirical factor. It is worth noting that the [OM]/[OC] ratio is site dependent. The [OM]/[OC] ratio of freshly emitted aerosols is usually smaller than that of the more aged (oxygenated) aerosols. In this study where a value of 1.4 is applied to this factor, it can be seen from Table 18 that the reconstructed masses at all the sites agree very well with the measured masses.

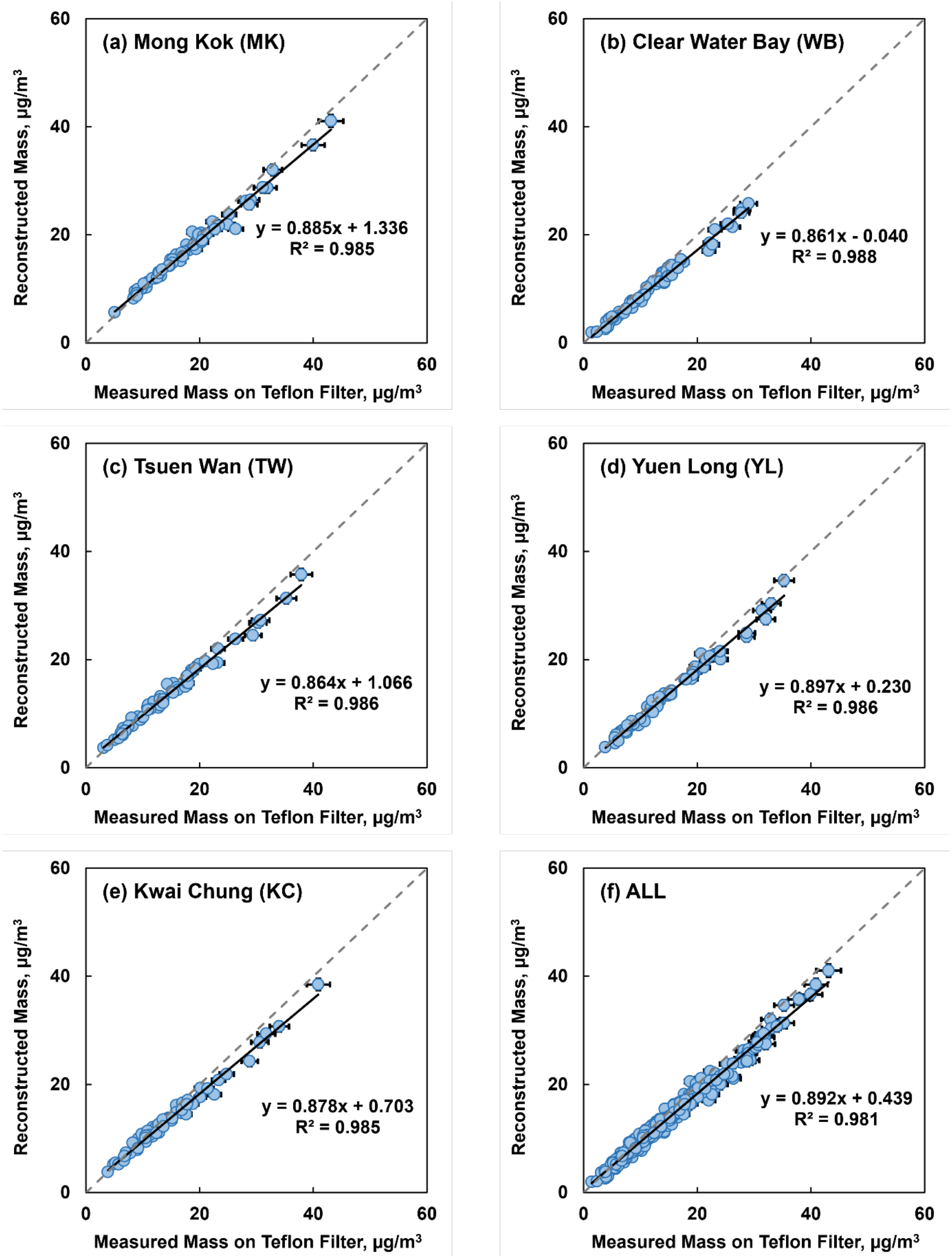

Figure 11. Scatter plots of reconstructed mass versus measured mass on Teflon filters for $PM_{2.5}$ samples collected at (a) MK, (b) WB, (c) TW, (d) YL, (e) KC, and (f) all sites.

Table 18. Statistics analysis of reconstructed mass versus measured mass on Teflon filters for $PM_{2.5}$ samples collected in this study (Quotation Ref. 21-02409)

Statistics/Site	MK	WB	TW	YL	KC	ALL
n	60	61	57	61	61	300
Slope	0.885 (±0.014)	0.861 (±0.012)	0.864 (±0.014)	0.897 (±0.014)	0.878 (±0.014)	0.892 (±0.007)
Intercept	1.336 (±0.279)	-0.040 (±0.179)	1.066 (±0.227)	0.230 (±0.235)	0.703 (±0.23)	0.439 (±0.121)
R^2	0.985	0.988	0.986	0.986	0.985	0.981
AVG Rec. Mass	17.08	10.82	13.74	13.72	13.59	13.78
AVG Mea. Mass	17.80	12.61	14.67	15.04	14.67	14.95
AVG Rec./Mea. Mass	0.975 (±0.058)	0.863 (±0.093)	0.960 (±0.076)	0.918 (±0.062)	0.940 (±0.066)	0.930 (±0.082)

The annual average composition (%) of the major components to the $PM_{2.5}$ mass is shown in Figure 12 for individual sites. Overall, the reconstructed mass agrees very well with the measured mass using an [OM]-to-[OC] ratio of 1.4.

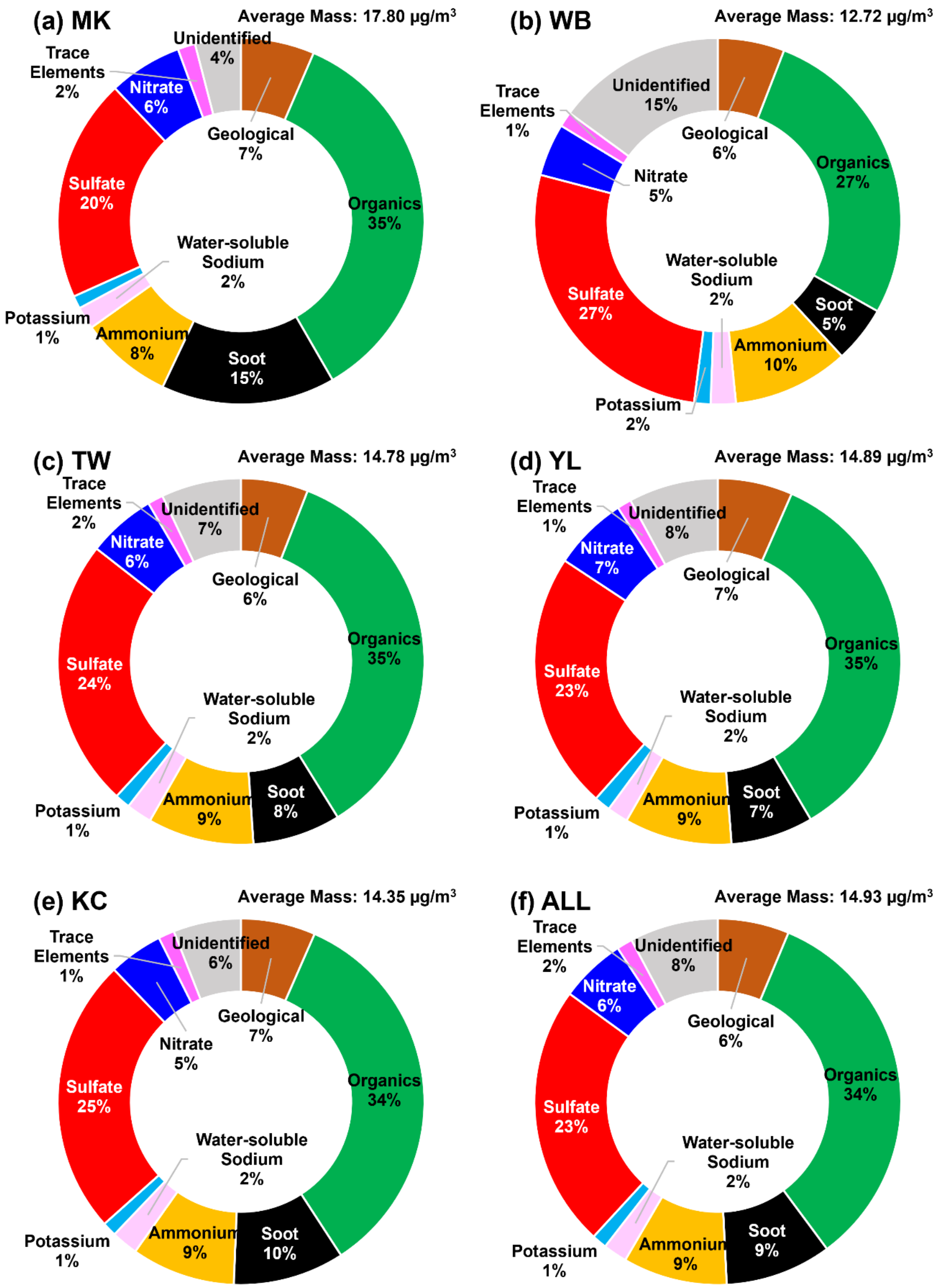

Figure 12. Annual average composition (%) of major components including 1) geological material; 2) organic matter; 3) soot; 4) ammonium; 5) water-soluble sodium; 6) potassium; 7) sulfate; 8) nitrate; 9) non-crustal trace elements, and 10) unidentified material (difference between measured mass and the reconstructed mass) to $PM_{2.5}$ mass for (a) MK, (b) WB, (c) TW, (d) YL, (e) KC, and (f) all sites.

On an annual average basis, MK had the highest $PM_{2.5}$ loading while WB had the lowest (Figure 13). For all of the five sites, sulfate and OM were the two most abundant components followed by ammonium and soot (EC by TOR method). The EC concentration was the highest at MK and the lowest at WB, which is consistent with their respective site characteristics (roadside vs. suburban locations). The concentrations of geological materials, ammonium, water-soluble sodium, potassium, sulfate and nitrate did not vary much across all five sites.

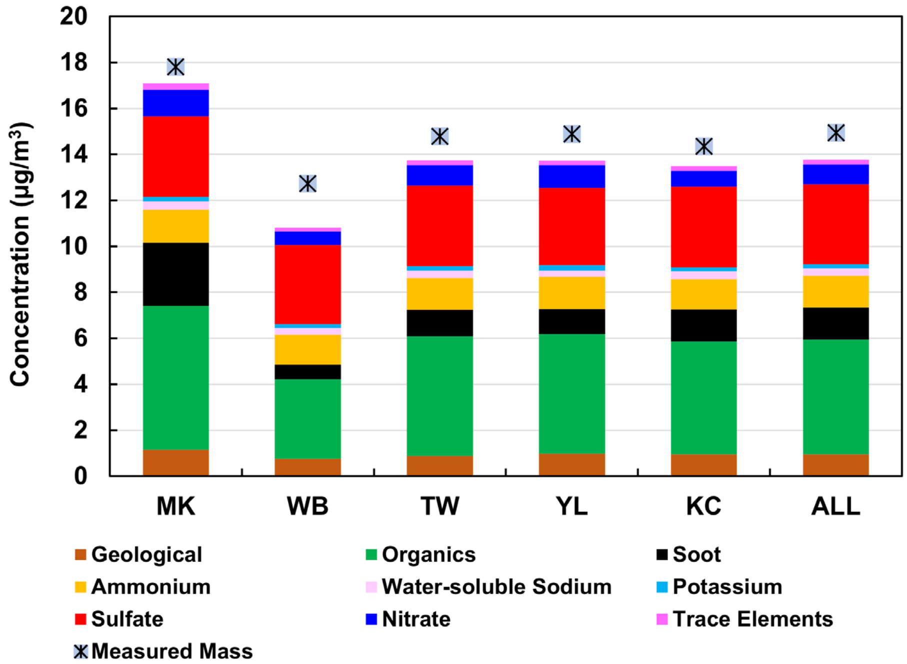

Figure 13. Comparison of annual average concentrations of major components including 1) geological material; 2) organic matter; 3) soot; 4) ammonium; 5) water-soluble sodium; 6) potassium; 7) sulfate; 8) nitrate, and 9) non-crustal trace elements and the $PM_{2.5}$ mass between individual sites.

3.3.6 Analysis of Collocated Data

In the Hong Kong $PM_{2.5}$ speciation network, two sites were equipped with collocated samplers during 2022, as shown in Table 2. The MK site included a third BGI PQ200 sampler for collecting Teflon filters while the WB site included a third BGI PQ200 sampler for collecting quartz fiber filters. The collocated samplers were operated on a 1-in-6 day schedule as the primary samplers did.

Figures 14–21 show examples of the comparisons for $PM_{2.5}$ mass concentration by gravimetric analysis, potassium, calcium, and iron by ED-XRF, ammonium and sulfate by IC, OC and EC by the TOR method, respectively. The least-squares linear regression parameters (slope, intercept, and R^2) by sites for each of these species are also included in the tables placed right below the respective figures (Tables 19–26). These figures demonstrate good to excellent agreement for the major analytes.

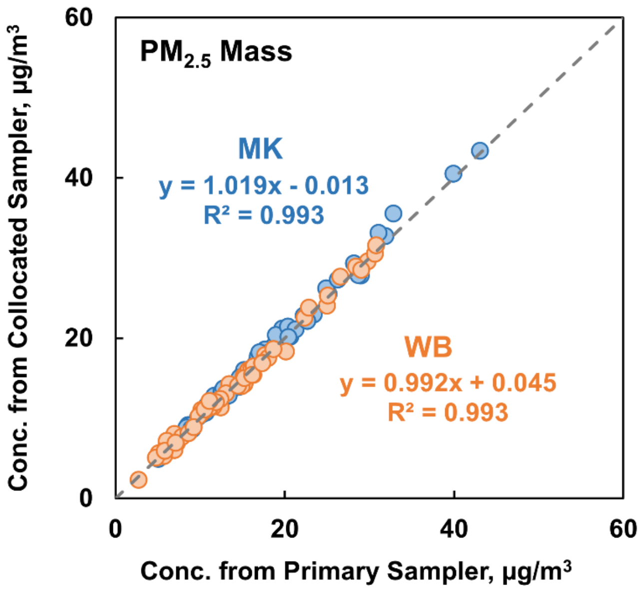

Figure 14. Collocated data for $PM_{2.5}$ concentrations at MK and WB sites during 2022.

Table 19. Statistics analysis of collocated data for $PM_{2.5}$ concentrations at MK and WB sites during 2022

Statistics/Site	MK	WB
n	60	61
Slope	1.019 (±0.011)	0.992 (±0.011)
Intercept	-0.013 (±0.215)	0.045 (±0.180)
R^2	0.993	0.993

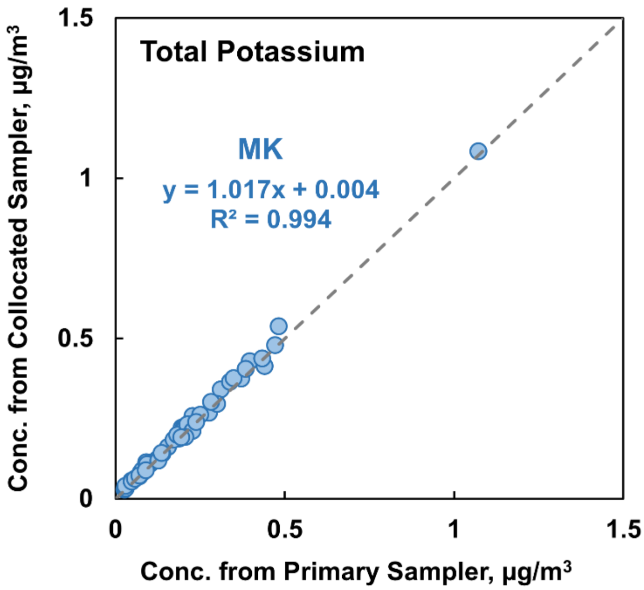

Figure 15. Collocated data for total potassium concentrations at MK site during 2022.

Table 20. Statistics analysis of collocated data for potassium concentrations at MK site during 2022

Statistics/Site	MK
n	60
Slope	1.017 (±0.010)
Intercept	0.004 (±0.003)
R^2	0.994

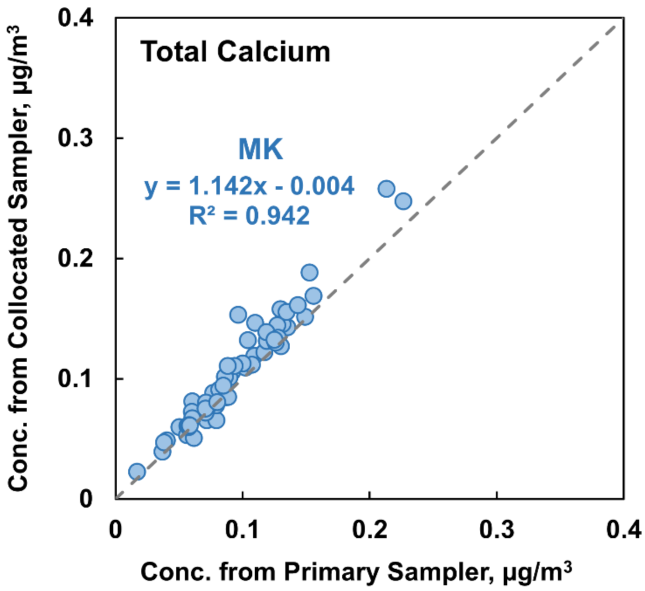

Figure 16. Collocated data for calcium concentrations at MK site during 2022.

Table 21. Statistics analysis of collocated data for calcium concentrations at MK site during 2022

Statistics/Site	MK
n	60
Slope	1.142 (±0.037)
Intercept	-0.004 (±0.004)
R^2	0.942

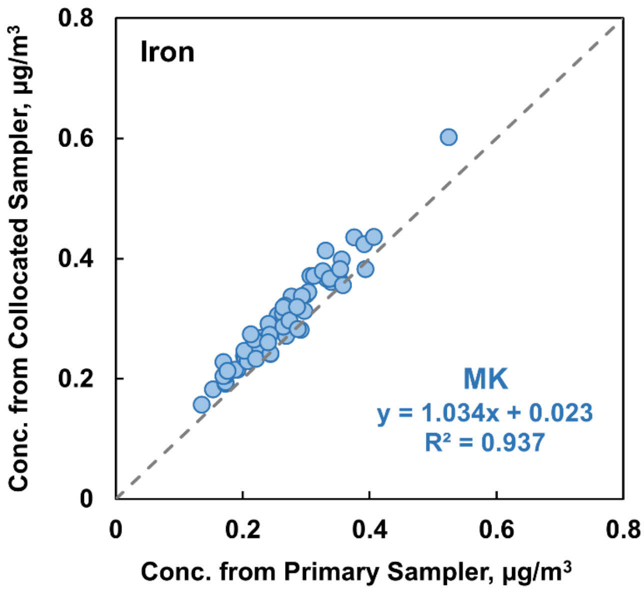

Figure 17. Collocated data for iron concentrations at MK site during 2022.

Table 22. Statistics analysis of collocated data for iron concentrations at MK site during 2022

Statistics/Site	MK
n	60
Slope	1.034 (±0.035)
Intercept	0.023 (±0.010)
R^2	0.937

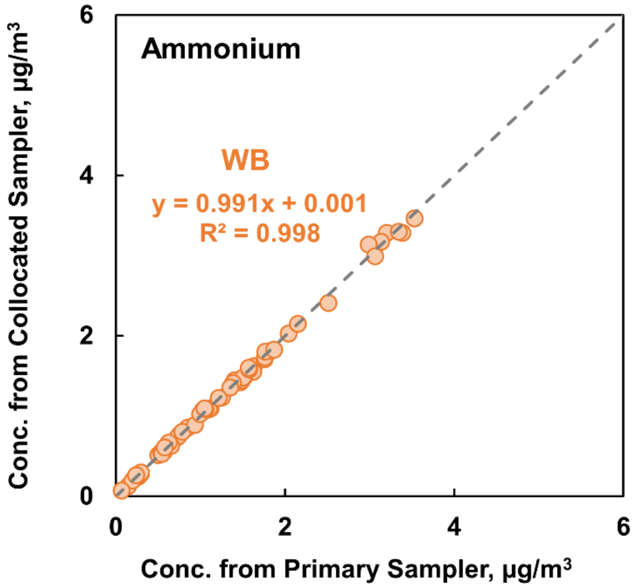

Figure 18. Collocated data for ammonium concentrations at WB site during 2022.

Table 23. Statistics analysis of collocated data for ammonium concentrations at WB site during 2022

Statistics/Site	WB
n	61
Slope	0.991 (±0.006)
Intercept	0.001 (±0.009)
R^2	0.998

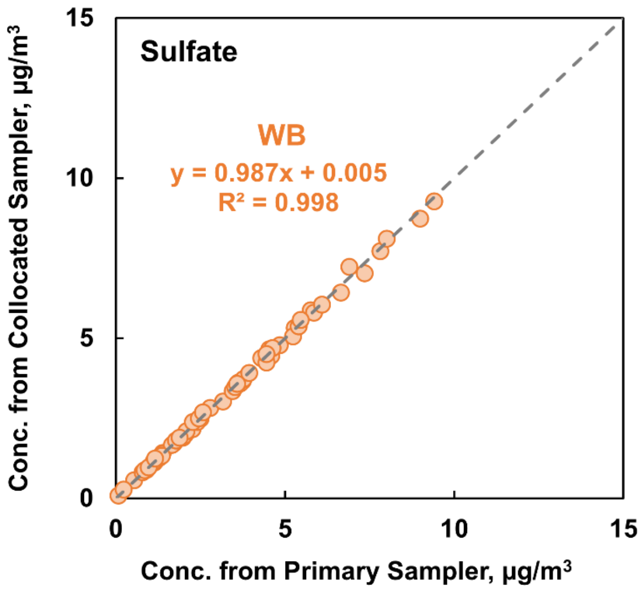

Figure 19. Collocated data for sulfate concentrations at WB site during 2022.

Table 24. Statistics analysis of collocated data for sulfate concentrations at WB site during 2022

Statistics/Site	WB
n	61
Slope	0.987 (±0.006)
Intercept	0.005 (±0.023)
R^2	0.998

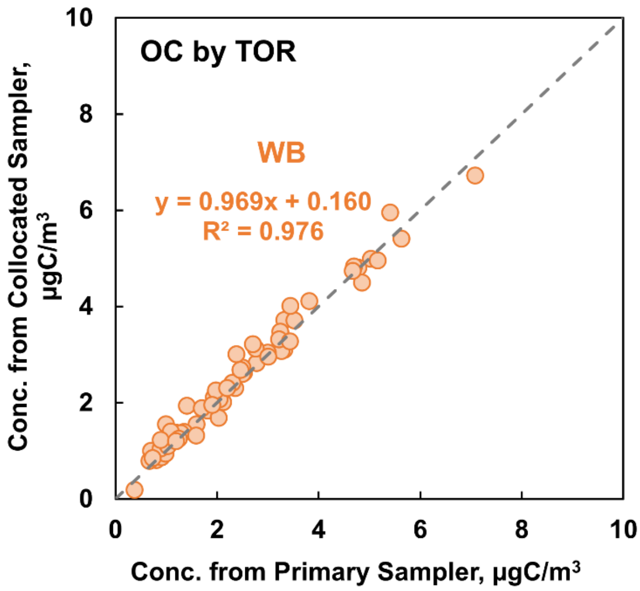

Figure 20. Collocated data for TOR OC concentrations at WB site during 2022.

Table 25. Statistics analysis of collocated data for TOR OC concentrations at WB site during 2022

Statistics/Site	WB
n	61
Slope	0.969 (±0.020)
Intercept	0.160 (±0.058)
R^2	0.976

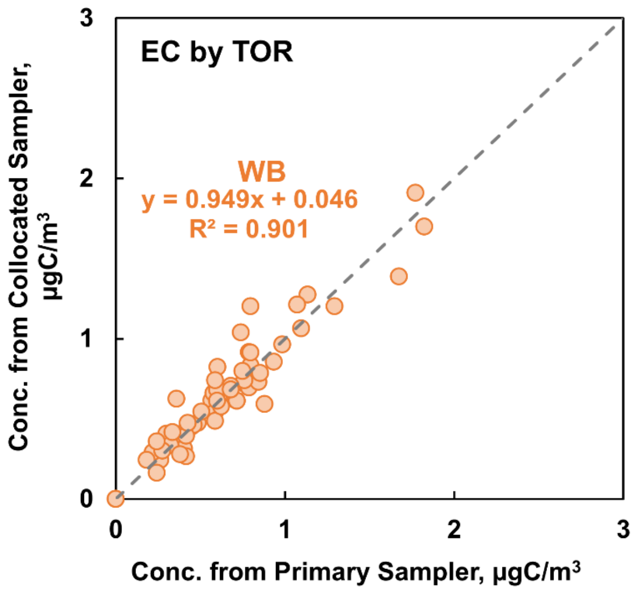

Figure 21. Collocated data for TOR EC concentrations at WB site during 2022.

Table 26. Statistics analysis of collocated data for TOR EC concentrations at WB site during 2022

Statistics/Site	WB
n	61
Slope	0.949 (±0.041)
Intercept	0.046 (±0.030)
R^2	0.901

3.3.7 $PM_{2.5}$ Mass Concentrations: Gravimetric vs. Continuous Measurements

Continuous monitoring of $PM_{2.5}$ concentrations were conducted at four monitoring sites by HKEPD during 2022. TEOMs (Tapered Element Oscillating Microbalance) are installed at MK YL, KC and TW sites. Comparisons of $PM_{2.5}$ mass concentrations from gravimetric measurement and 24-hr average TEOM/beta gauge measurement were conducted. The results are presented in both time-series plots and scatter plots (Figure 22). The two types of measurements show good agreement (R^2 = 0.86–0.98) with slopes ranging from 0.944 at TW site to 1.063 at KC site.

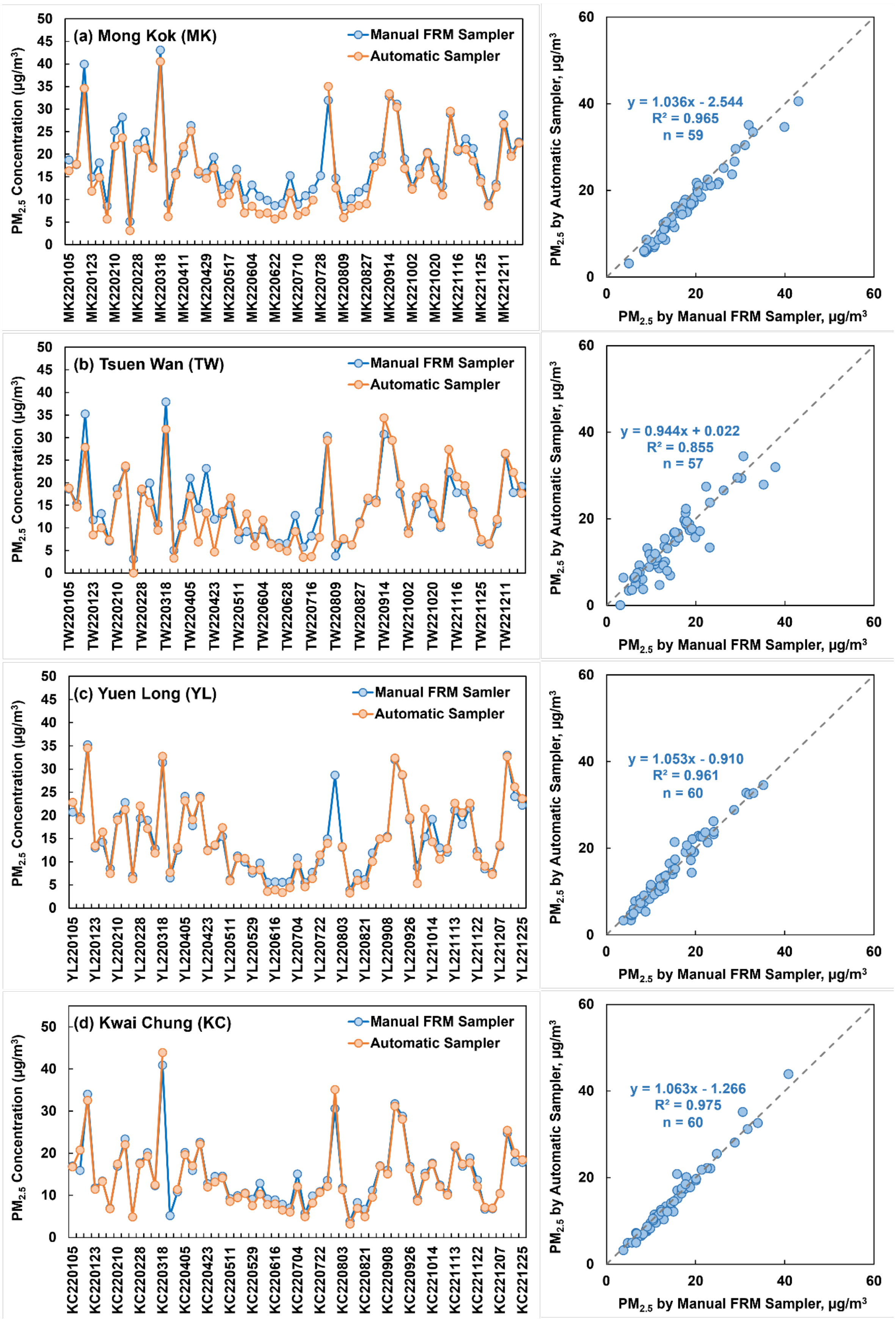

Figure 22. Comparisons of $PM_{2.5}$ mass concentrations from gravimetric and continuous measurements at (a) MK, (b) TW, (c) YL, and (d) KC sites during 2022.

4. $PM_{2.5}$ Annual Trend and Seasonal Variation

4.1 $PM_{2.5}$ Annual Trend

A side-by-side comparison of the annual average $PM_{2.5}$ concentration and chemical composition data is shown in Appendix A [Chow et al., 2002, 2006, 2010, 2016, 2019; Yu et al., 2012, 2013, 2014, 2015, 2017, 2018; Watson et al., 2021, 2022]. The MK and TW sites have data since 2000, the YL site has data since 2004, the WB site has data since 2011, the CW and TC sites have data during 2011–2016, the KC site started operation from May 2014, while no data is available from the Hok Tsui (HT) site after 2009.

Compared to the year of 2021, the annual average $PM_{2.5}$ concentration at all sites exhibited a decrease of 1.98–3.14 $\mu g/m^3$ corresponding to a 11.6-16.5% reduction.

Annual trends of $PM_{2.5}$ mass were examined for MK, WB, TW, and YL sites across the years when data are available (Figure 23). The Mann-Kendall non-parametric statistical test (MK test) [Salmi et al., 2002; Sen, 1968] was applied to the dataset and shows a monotonic decreasing trend at 95% confidence interval across all four sites during 2011–2022. The Sen's slopes for annual average $PM_{2.5}$ concentrations are -2.27, -1.48, -1.65, and -1.71 $\mu g/m^3$/year at MK, WB, TW, and YL sites, respectively (Table 27).

Measured species were grouped into nine categories for better comparison (Figure 24). Note that no sampling was conducted at TW site from October to December in 2019 due to the renovation at the site. For OC at MK, TW and YL sites, high concentration levels were observed in the first two studies (i.e. 2000–01 and 2004–05) and then the concentrations maintained at lower levels since 2008. At all four sites, the EC concentrations follow a broadly decline trend from 2011 to 2022. A statistical summary of the MK test and Sen's slopes for all the individual major components in $PM_{2.5}$ at MK, WB, TW and YL sites during 2011–2022 is also given in Table 26. Geological material, ammonium, potassium, sulfate and non-crustal trace elements exhibited a monotonic decreasing trend at 95% confidence interval at all four sites. On the other hand, water-soluble sodium and nitrate did not consistently show a monotonic decreasing trend at all four sites during the same time window.

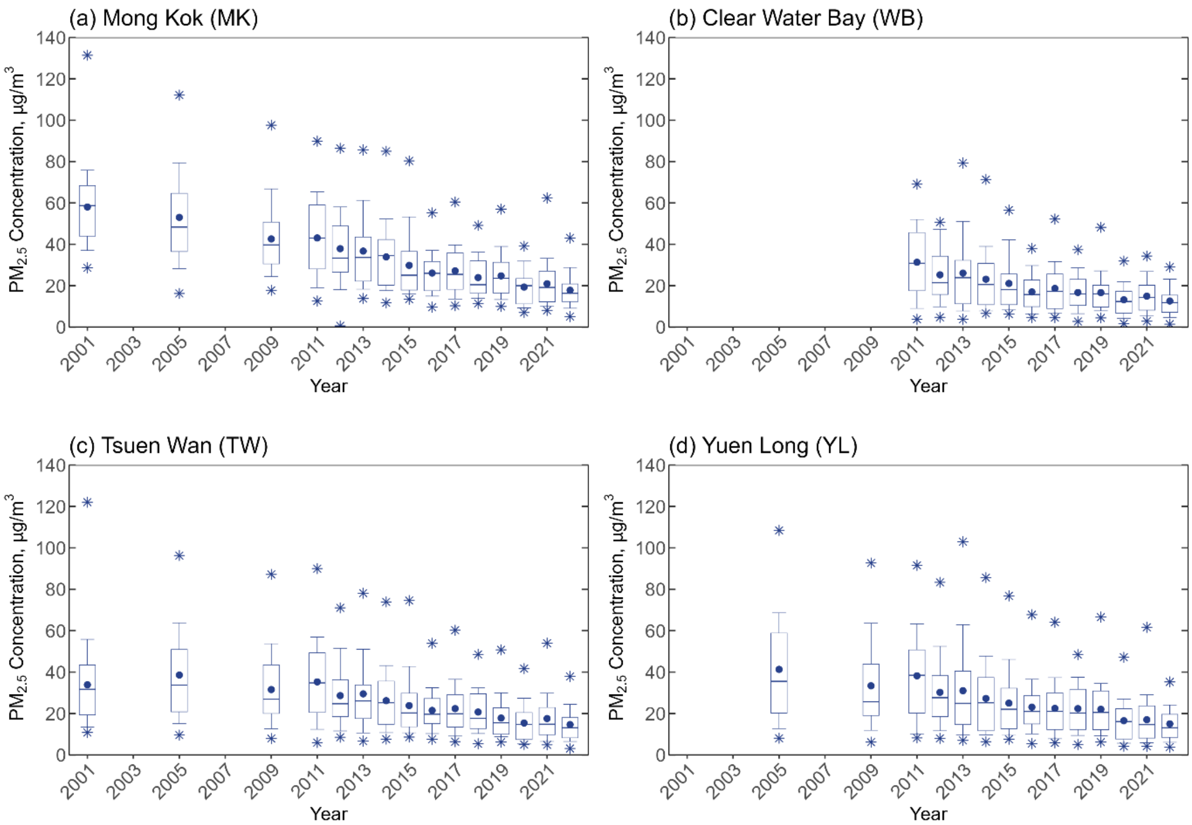

Figure 23. Comparisons of annual average $PM_{2.5}$ mass concentrations at (a) MK, (b) WB, (c) TW, and (d) YL sites from 2000 to 2022 (wherever data are available) (Bottom and top of box: the 25th and 75th percentiles; whiskers: the 10th and 90th percentiles; dot in the box: the average; line in the box: the median; asterisks: the minimum and maximum values).

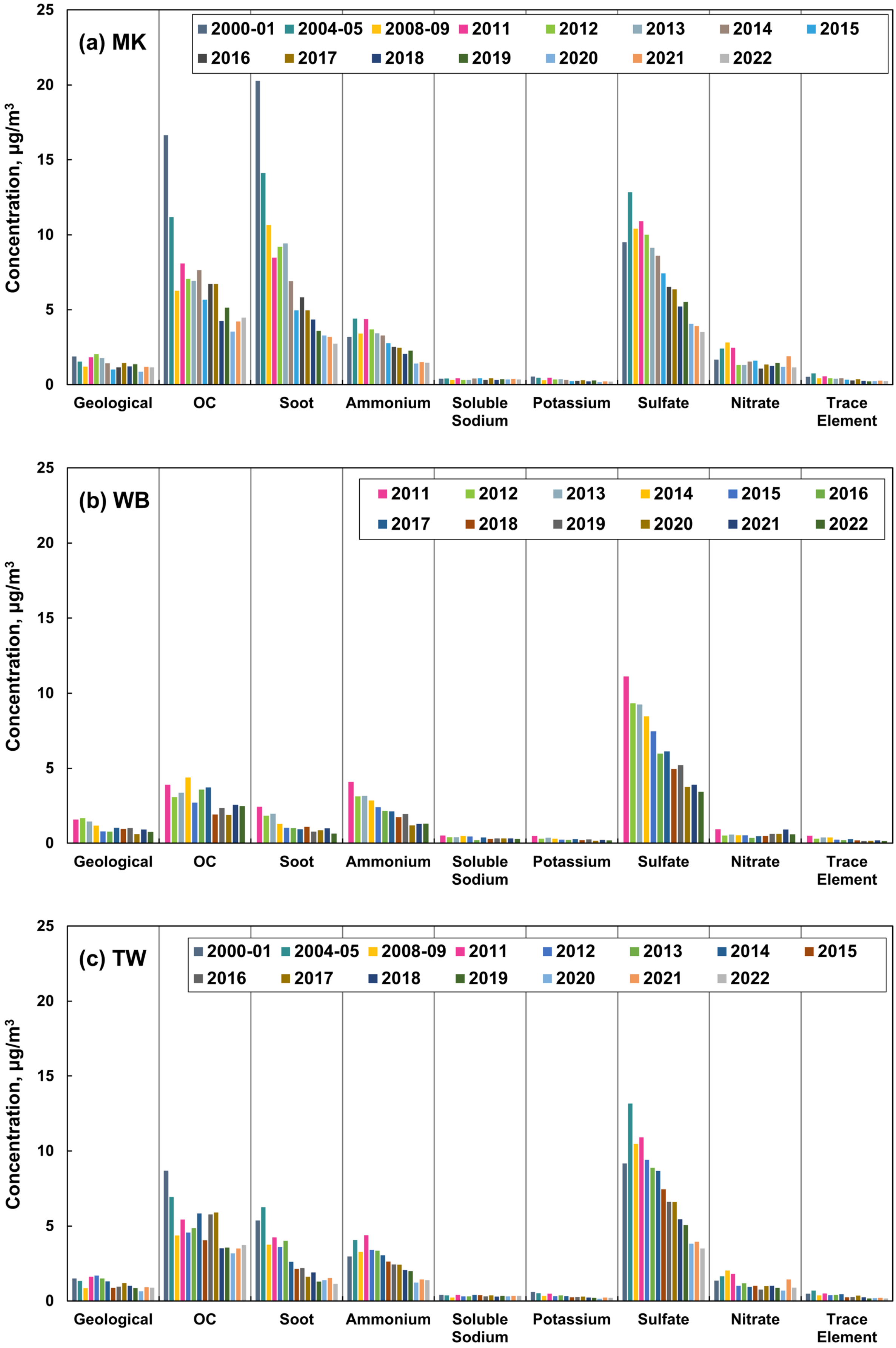

(a) MK
2000-01
2004-05
2008-09
2011
2012
2013
2014
2015
2016
2017
2018
2019
2020
2021
2022
(b) WB
(c) TW
Concentration, μg/m³
25
20
15
10
5
0
Geological
OC
Soot
Ammonium
Soluble Sodium
Potassium
Sulfate
Nitrate
Trace Element

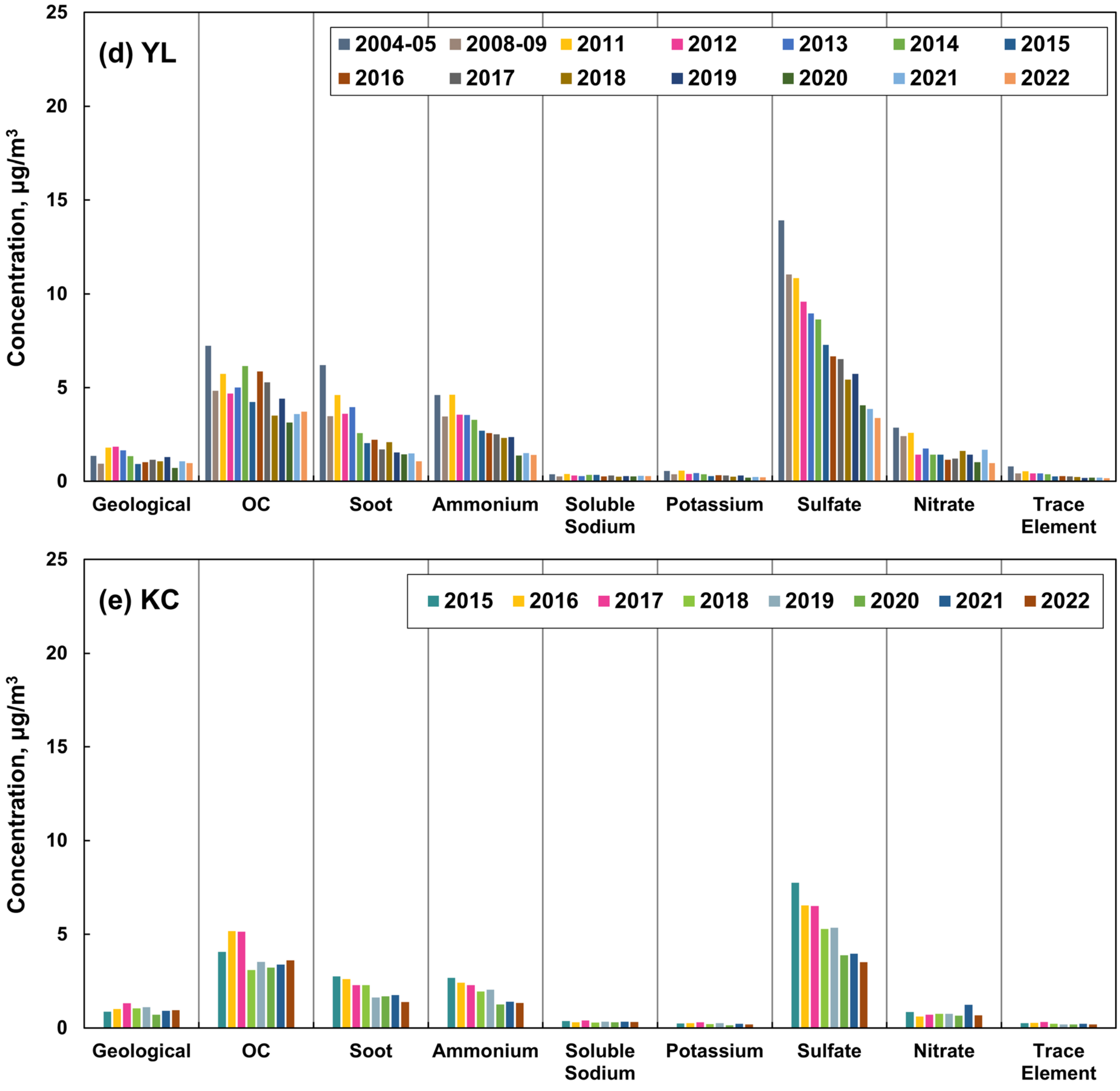

Figure 24. Annual trends of major components of $PM_{2.5}$ samples collected at (a) MK, (b) WB, (c) TW, (d) YL and (e) KC sites from 2000 to 2022 (wherever data are available).

Table 27. Statistical summary of the Mann-Kendall test (at 95% confidence interval) and Sen's slopes for the major components in the $PM_{2.5}$ at MK, WB, TW and YL sites during 2011–2022

	Geological	OC	Soot	Ammonium	Sodium ion	Potassium	Sulfate	Nitrate	Trace Element	$PM_{2.5}$
					MK					
MK test p-value	0.0082	0.0010	0.0000	0.0000	0.5000	0.0010	0.0000	0.1518	0.0037	0.0000
MK test trend	downward	downward	downward	downward	no	downward	downward	no	downward	downward
Sen slope (μg/m^3/year)	-0.066	-0.372	-0.590	-0.256	0.000	-0.018	-0.677	-0.019	-0.021	-2.266
					WB					
MK test p-value	0.0025	0.0234	0.0004	0.0001	0.0118	0.0010	0.0000	0.3156	0.0016	0.0000
MK test trend	downward	downward	downward	downward	downward	downward	downward	no	downward	downward
Sen slope (μg/m^3/year)	-0.074	-0.142	-0.118	-0.238	-0.018	-0.018	-0.667	0.008	-0.024	-1.477
					TW					
MK test p-value	0.0025	0.0432	0.0001	0.0000	0.2253	0.0004	0.0000	0.0574	0.0025	0.0000
MK test trend	downward	downward	downward	downward	no	downward	downward	no	downward	downward
Sen slope (μg/m^3/year)	-0.076	-0.172	-0.268	-0.234	-0.005	-0.018	-0.666	-0.031	-0.024	-1.650
					YL					
MK test p-value	0.0082	0.0234	0.0001	0.0000	0.0234	0.0002	0.0000	0.0168	0.0004	0.0000
MK test trend	downward	downward	downward	downward	downward	downward	downward	downward	downward	downward
Sen slope (μg/m^3/year)	-0.078	-0.195	-0.253	-0.247	-0.008	-0.023	-0.648	-0.056	-0.027	-1.707

4.2 Seasonal Variation of $PM_{2.5}$ in 2022

Monthly average $PM_{2.5}$ concentration and chemical compositions for individual sites are shown in Figure 25. Higher $PM_{2.5}$ concentrations were recorded in January through March and December, primarily due to elevated levels of sulfate, nitrate, ammonium, and organics. The highest daily $PM_{2.5}$ concentration (43.10 µg/m^3) appeared at MK on 18 March, 2022. On this day, TW and KC sites also had the highest daily $PM_{2.5}$ while WB and YL experienced the second (27.90 µg/m^3) and the fourth highest daily $PM_{2.5}$ (31.40 µg/m^3), respectively. This result indicated a regional pollution episode brought in by northwesterly wind. The prevailing wind shifted from northwesterly in winter to southeasterly in summer, resulting in clean marine air diluting pollutants and improved air quality in the months of June and July. Notably, the daily $PM_{2.5}$ concentration of the samples collected on 2, 8, and 26 September (ranging from 14.22-19.77 µg/m^3) were comparable with the values in late August (3.99-11.90 µg/m^3), but increased to a range of 26.68-32.89 µg/m^3 on 14 and 20 September due to the elevated levels of sulfate, nitrate, ammonium, and organics. This increase led to September being the highest monthly averaged $PM_{2.5}$ in 2022.

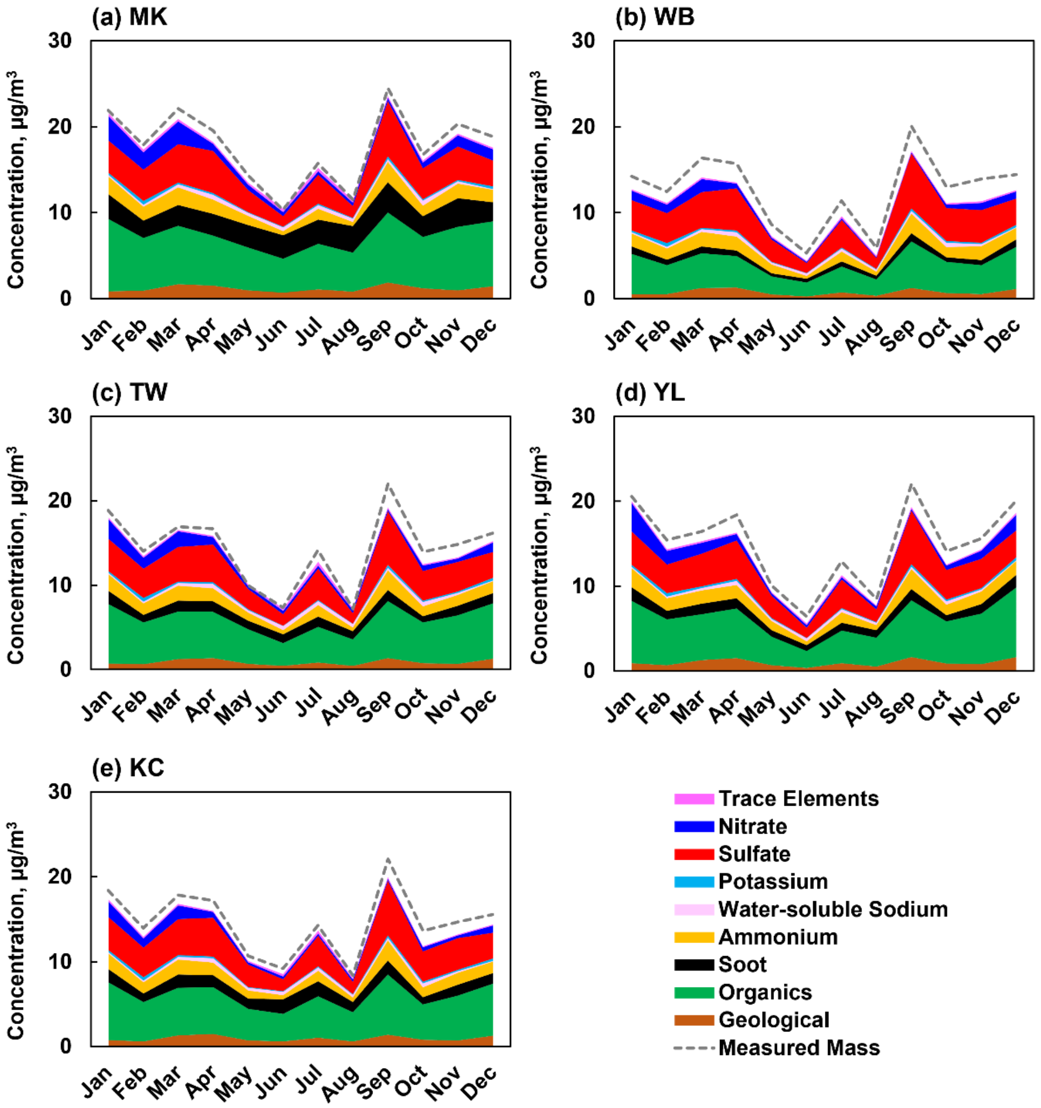

Figure 25. Monthly average of $PM_{2.5}$ mass concentrations and chemical compositions for (a) MK, (b) WB, (c) TW, (d) YL, and (e) KC during 2022 $PM_{2.5}$ speciation study.

5. Summary

This data summary report covers the validation and quality assurance aspects of the chemical analysis of filter samples from the Hong Kong $PM_{2.5}$ speciation network from January 1 through December 31, 2022. Sampling was conducted at MK, WB, TW, YL, and KC sites on a 1-in-6 day schedule which yielded a total of 61 sampling events through the year.

All of the 870 $PM_{2.5}$ filter samples received are considered valid after Level I data validation. Therefore, all the samples (726 $PM_{2.5}$ samples and 144 field blanks) were submitted for comprehensive chemical analyses. The laboratory accuracy and precision were within limits as demonstrated by routine QC samples.

Three levels of validation were performed on the complete dataset. Reconstructed mass and measured mass are highly correlated with correlation coefficients (R^2) of 0.98 at all individual sites. It further supports the validity of both gravimetric analysis and chemical measurements. The reconstructed mass and the measured mass were in excellent agreement.

In 2022, the highest annual average $PM_{2.5}$ concentration of 17.80 μg/m^3 was measured at the roadside MK site. The lowest annual average $PM_{2.5}$ concentration of 12.72 μg/m^3 was recorded at the suburban WB site. The $PM_{2.5}$ concentrations at all the five monitoring sites were within the existing AQO annual $PM_{2.5}$ standard of 25 μg/m^3 and 24-hr average limit of 50 μg/m^3.

Similar to the past years, organics (assuming to be 1.4×OC) and sulfate represented the most abundant components in the $PM_{2.5}$ across all the five sites. The relative importance of these two components varied with the sampling sites. Organics, with contributions from both primary emission sources (e.g., vehicular exhaust, biomass burning) and secondary formation from a myriad of volatile and semivolatile organic compound precursors, showed the largest percentage contribution of 35% at MK site (vs. 20% for sulfate). Similarly, organics was the most abundant component at TW, YL, and KC site (34-35%), followed by sulfate formed from atmospheric oxidation of sulfur dioxide (23-25%). These two major components had similar percentage shares at WB sites (27% for both organics and sulfate).

Nitrate, formed from atmospheric oxidation of nitrogen oxides, was much lower than sulfate, contributing 5–7% to the total fine PM masses at all the sampling sites. Ammonium, forming from ammonia (the most abundant alkaline gas in the atmosphere), was reasonably balanced by sulfate and nitrate and it existed dominantly as ammonium sulfate across all the sampling sites in the year of 2022. This component made up 8–10% of $PM_{2.5}$ mass at all the sampling sites. EC, exclusively from combustion sources, exhibited a clear roadside-urban-suburban gradient pattern with the highest annual average concentration observed at MK site (2.73 μgC/m^3, 15% of the $PM_{2.5}$ mass) and the lowest annual average concentration at WB site (0.64 μgC/m^3, 5% of the $PM_{2.5}$ mass).

Hong Kong experienced higher $PM_{2.5}$ levels during fall and winter months (Jan, Feb, Mar, Sep, Oct, Nov, and Dec) while summer months (Jun–Aug) usually have lower $PM_{2.5}$ concentrations. The extra mass between the high and low $PM_{2.5}$ concentrations was mainly attributed to ammonium sulfate, ammonium nitrate and organics which usually exhibited high concentrations simultaneously across all five sites, suggesting that regional sources were the most probable $PM_{2.5}$ contributors on high $PM_{2.5}$ concentration days. On the other hand, the lack of temporal variation for EC concentrations at individual site, together with the aforementioned roadside-urban-suburban gradient pattern, suggested that local sources (e.g. on-road vehicles) were its major contributors. While a wide range of measures taken by the HKSAR Government to control the vehicular emissions have proved to be effective and responsible for the general decreasing trend of EC levels observed at roadside, continuous efforts are needed to contain the air pollution at lower levels so as to keep compliance with the existing AQO criteria.

Moreover, the meteorological conditions (especially wind speed and direction) have a large influence on the PM levels measured in Hong Kong. Lower $PM_{2.5}$ concentrations were observed during June–August when the southerly winds prevailed and brought in clean maritime air while higher $PM_{2.5}$ concentrations were usually associated with northeasterly winds which carried regional pollutants into Hong Kong.

Compared to the year of 2021, the annual average $PM_{2.5}$ concentration at all sites exhibited a decrease of 1.98–3.14 $\mu g/m^3$ or 11.6-16.5%; The Mann-Kendall non-parametric statistical test shows a continuing downward trend in overall $PM_{2.5}$ concentrations in Hong Kong over the 2011–2022 period, indicating that the general air quality in Hong Kong is improving.

References

Air Quality Research Center of the UC-Davis (2022), UCD CSN Standard Operating Procedure #402: Thermal/Optical Reflectance (TOR) Carbon Analysis Using a Sunset Carbon Analyzer. Available at: https://airquality.ucdavis.edu/sites/g/files/dgvnsk1671/files/inline-files/CSN_SOP_402_v1.3_TOR_Carbon_Analysis_%28Sunset_5L%29.pdf

Air Quality Research Center of the UC-Davis (2023), Chemical Speciation Network (CSN) Annual Quality Report: Samples Collected January 1, 2021 through December 31, 2021. Available at: https://airquality.ucdavis.edu/sites/g/files/dgvnsk1671/files/inline-files/CSN_2021AnnualQualityReport.pdf

Bevington, P. R. (1969), Data Reduction and Error Analysis for the Physical Sciences, MaGraw Hill, New York, NY.

Birch, M. E. and R. A. Cary (1996), Elemental carbon-based method for monitoring occupational exposures to particulate diesel exhaust, *Aerosol Sci. Technol.*, 25, 221-241.

European Committee for Standardization (2017). Ambient air: measurement of elemental carbon (EC) and organic carbon (OC) collected on filters. Brussels (BS EN 16909:2017).

Chen, L. -W. A., J. C. Chow, J. G. Watson, H. Moosmüller, and W. P. Arnott (2004), Modeling reflectance and transmittance of quartz-fiber filter samples containing elemental carbon particles: Implications for thermal/optical analysis, *J. Aerosol Sci.*, 35, 765-780.

Chow, J. C., J. G. Watson, L. C. Pritchett, W. R. Pierson, C. A. Frazier, and R. G. Purcell (1993), The DRI thermal/optical reflectance carbon analysis system: description, evaluation and applications in U. S. air quality studies, *Atmos. Environ.*, 27A, 1185-1201.

Chow, J. C., J. G. Watson, L. -W. A. Chen, W. P. Arnott, H. Moosmüller, and K. K. Fung (2004), Equivalence of elemental carbon by Thermal/Optical Reflectance and Transmittance with different temperature protocols, *Environ. Sci. Technol.*, 38, 4414-4422.

Chow, J. C., J. G. Watson, L. -W. A. Chen, M. C. O. Chang, N. F. Robinson, D. Trimble, and S. D. Kohl (2007), The IMPROVE_A temperature protocol for thermal/optical carbon analysis: maintaining consistency with a long-term database, *J. Air Waste Manage. Assoc.*, 57, 1014-1023.

Chow, J. C., J. G. Watson, Kohl, S. D., Gonzi, M. P., L. -W. A. Chen (2002), Measurements and Validation for the Twelve Month Particulate Matter Study in Hong Kong, available at: http://www.epd.gov.hk/epd/english/environmentinhk/air/studyrpts/files/final_version_hkepdfinalreport_rev12-12-02.pdf.

Chow, J. C., J. G. Watson, Kohl, S. D., Voepel, H. E., L. -W. A. Chen (2006), Measurements and Validation for the Twelve Month Particulate Matter Study in Hong Kong, available at: http://www.epd.gov.hk/epd/english/environmentinhk/air/studyrpts/files/HKEPDFinalReportRev_V8.pdf.

Chow, J. C., J. G. Watson, Kohl, S. D., L. -W. A. Chen (2010), Measurements and validation of the 2008/2009 particulate matter study in Hong Kong, available at: http://www.epd.gov.hk/epd/english/environmentinhk/air/studyrpts/files/HKEPDFinalReportRev_11-29-10_v2.pdf.

Chow, J. C., J. G. Watson, P. M. Cropper, X. Wang, and S. D. Kohl (2016), Fine Particulate Matter ($PM_{2.5}$) Sample Chemical Analysis January 1, 2015 – December 31, 2015, available at HKEPD website: http://www.epd.gov.hk/epd/sites/default/files/epd/english/environmentinhk/air/studyrpts/files/final_report_mvtmpms_2015.pdf.

Chow, J. C., J. G. Watson, M. C. Green, X. Wang, and S. D. Kohl (2019), Fine Particulate Matter ($PM_{2.5}$) Sample Chemical Analysis January 1, 2018 – December 31, 2018, available at HKEPD website: https://www.epd.gov.hk/epd/sites/default/files/epd/english/environmentinhk/air/studyrpts/files/final_report_mvtmpms_2018.pdf.

Hong Kong Observatory (HKO) (2013), The year's weather – 2013, Climatological Publications, available at: http://www.weather.gov.hk/wxinfo/pastwx/ywx2013.htm.

Research Triangle Institute (RTI) (2005), Data validation process for the $PM_{2.5}$ Chemical Speciation Network, Prepared for Center for Environmental Measurements and Quality Assurance, USEPA.

Salmi, T., A. Määttä, P. Anttila, T. Ruoho-Airola, and T. Amnell (2002), Detecting trends of annual values of atmospheric pollutants by the Mann-Kendall test and Sen's slope estimates – the excel template application MAKESENS, Finnish Meteorological Institute, Helsinki.

Sen, P. K. (1968), Estimates of the regression coefficient based on Kendall's Tau, *J. Am. Stat. Assoc.*, 63, 1379-1389.

U. S. Environmental Protection Agency (USEPA) (1999), Particulate Matter ($PM_{2.5}$) Speciation Guidance, available at: http://www.epa.gov/ttnamti1/files/ambient/pm25/spec/specfinl.pdf.

U. S. Environmental Protection Agency (USEPA) (2012), Quality Assurance Guidance Document for $PM_{2.5}$ Chemical Speciation Sampling at Trends, NCore, Supplemental and Tribal Sites, available at: http://www.epa.gov/ttnamti1/files/ambient/pm25/spec/CSN_QAPP_v120_05-2012.pdf.

Watson, J. G., J. C. Chow, and C. A. Frazier (1999), X-ray fluorescence analysis of ambient air samples, Elemental Analysis of Airborne Particles, Vol 1, by S. Landsberger and M. Creatchman, Eds. Gordon and Breach Science, Amsterdam, 67-96.

Watson, J. G., B. J. Turpin, and J. C. Chow (2001), The measurement process: Precision, accuracy, and validity, in *Air Sampling Instrument for Evaluation for Atmospheric Contaminants*, 9th ed., B. S. Cohen and C. S. J. McCammon, Eds. American Conference of Governmental Industrial Hygienists, Cincinnati, OH, 201-216.

Watson, J.G., J. C. Chow, X. Wang, S.D. Kohl (2021), Fine Particulate Matter ($PM_{2.5}$) Sample Chemical Analysis January 1, 2020 – December 31, 2020, available at HKEPD website: https://www.epd.gov.hk/epd/sites/default/files/epd/english/business_job/business_opp/files/final_report_mvtmpms_2020.pdf

Watson, J.G., J. C. Chow, X. Wang, S.D. Kohl (2022), Fine Particulate Matter ($PM_{2.5}$) Sample Chemical Analysis January 1, 2021 – December 31, 2021, available at HKEPD website: https://www.epd.gov.hk/epd/sites/default/files/epd/english/environmentinhk/air/studyrpts/files/final_report_mvtmpms_2021.pdf.

Witz, S., R. W. Eden, M. W. Wadley, C. Dunwoody, R. P. Papa, and K. J. Torre (1990), Rapid loss of particulate nitrate, chloride and ammonium on quartz fiber filters during storage, *J. Air Waste Manage. Assoc.*, 40, 53-61.

Yu, J. Z., X. H. H. Huang, and W. M. Ng (2012), Final report for provision of service for fine particulate matter ($PM_{2.5}$) sample chemical analysis, available at HKEPD website: http://www.epd.gov.hk/epd/english/environmentinhk/air/studyrpts/files/final_report_mvtmpms_2011.pdf.

Yu, J. Z., X. H. H. Huang, and W. M. Ng (2013), Final report for provision of service for fine particulate matter ($PM_{2.5}$) sample chemical analysis, available at HKEPD website: http://www.epd.gov.hk/epd/english/environmentinhk/air/studyrpts/files/final_report_mvtmpms_2012.pdf.

Yu, J. Z., X. H. H. Huang, T. Zhang, and W. M. Ng (2014), Final report for chemical speciation of $PM_{2.5}$ filter samples, January 1 through December 31, 2013, available at HKEPD website: http://www.epd.gov.hk/epd/sites/default/files/epd/english/environmentinhk/air/studyrpts/files/final_report_mvtmpms_2013.pdf.

Yu, J. Z. and T. Zhang (2017), Final report for chemical speciation of $PM_{2.5}$ filter samples, January 1 through December 31, 2016, available at HKEPD website: http://www.epd.gov.hk/epd/sites/default/files/epd/english/environmentinhk/air/studyrpts/files/final_report_mvtmpms_2016.pdf.

Yu, J. Z. and T. Zhang (2018), Final report for chemical speciation of $PM_{2.5}$ filter samples, January 1 through December 31, 2017, available at HKEPD website: https://www.epd.gov.hk/epd/sites/default/files/epd/english/environmentinhk/air/studyrpts/files/final_report_mvtmpms_2017.pdf.

Appendix A. Annual average $PM_{2.5}$ concentration and chemical composition measured in Hong Kong during 2000–2022.

Site	MK															WB			
Year	2001	2005	2009	2011	2012	2013	2014	2015	2016	2017	2018	2019	2020	2021	2022	2011	2012	2013	2014
Teflon Mass	58.281	53.023	41.600	43.077	38.934	36.720	33.902	29.822	26.110	27.179	23.923	24.750	19.334	20.942	17.803	31.320	25.482	26.080	23.124
Quartz Mass	62.502	54.868	45.924	47.922	58.035	41.376	35.986	32.416	27.954	29.794	25.418	27.876	22.315	23.161	20.683	35.893	45.577	30.377	23.815
Cl-	0.256	0.283	0.312	0.205	0.102	0.119	0.203	0.226	0.114	0.191	0.107	0.135	0.157	0.165	0.167	0.105	0.067	0.093	0.123
NO3-	1.653	2.404	2.809	2.452	1.321	1.313	1.528	1.600	1.082	1.356	1.261	1.433	1.183	1.892	1.154	0.934	0.508	0.580	0.520
SO4=	9.502	12.840	10.414	10.912	10.015	9.142	8.604	7.425	6.525	6.356	5.211	5.523	4.047	3.911	3.501	11.128	9.338	9.246	8.452
NH4+	3.174	4.400	3.402	4.373	3.682	3.423	3.281	2.755	2.507	2.454	2.042	2.254	1.396	1.503	1.448	4.090	3.128	3.162	2.848
Na+	0.398	0.423	0.320	0.431	0.324	0.326	0.420	0.426	0.326	0.439	0.323	0.362	0.344	0.384	0.352	0.510	0.394	0.401	0.482
K+	0.457	0.479	0.278	0.467	0.349	0.319	0.286	0.190	0.223	0.235	0.173	0.219	0.106	0.137	0.139	0.483	0.288	0.318	0.273
OC	16.642	11.177	6.262	8.094	7.055	6.916	7.638	5.668	6.717	6.718	4.240	5.133	3.534	4.207	4.475	3.905	3.072	3.373	4.389
EC	20.288	14.115	10.661	8.481	9.199	9.421	6.905	4.959	5.833	4.946	4.339	3.576	3.272	3.181	2.733	2.431	1.843	1.963	1.289
TC	36.911	25.284	16.912	16.550	16.254	16.330	14.543	10.623	12.550	11.664	8.538	8.709	6.780	7.359	7.168	6.313	4.915	5.328	5.678
Al	0.1139	0.1408	0.0986	0.1942	0.2365	0.2034	0.1671	0.0885	0.1220	0.1472	0.1028	0.1319	0.035	0.075	0.098	0.1990	0.2260	0.2005	0.1686
Si	0.4778	0.3469	0.2485	0.3981	0.4393	0.3732	0.2760	0.1604	0.1993	0.2680	0.1883	0.2682	0.141	0.209	0.212	0.3980	0.4064	0.3527	0.2690
P	0.0092	0.1886	0.0225	0.0194	0.0211	0.0177	0.0188	0.0000	0.0044	0.0041	0.0000	0.0021	0.000	0.000	0.000	0.0150	0.0129	0.0124	0.0134
S	3.4886	4.3005	3.3471	3.6677	3.3455	3.1377	3.0873	2.8024	2.5718	2.5841	2.0758	2.3081	1.528	1.470	1.489	3.8399	3.1763	3.2338	3.0280
Cl	0.1169	0.1391	0.1037	0.0889	0.0386	0.0754	0.1303	0.1299	0.0620	0.1466	0.0978	0.0821	0.117	0.130	0.129	0.0720	0.0235	0.0954	0.1324
K	0.5517	0.4678	0.3064	0.4619	0.3447	0.3658	0.3136	0.2329	0.2464	0.3008	0.2150	0.2908	0.178	0.227	0.201	0.4740	0.3005	0.3690	0.3030
Ca	0.1705	0.1082	0.1102	0.1298	0.1461	0.1244	0.1061	0.1049	0.0959	0.1216	0.1128	0.1004	0.092	0.111	0.096	0.0914	0.1090	0.0853	0.0722
Ti	0.0092	0.0109	0.0109	0.0128	0.0147	0.0126	0.0099	0.0086	0.0086	0.0103	0.0114	0.0088	0.008	0.010	0.009	0.0106	0.0116	0.0103	0.0078
V	0.0134	0.0190	0.0175	0.0146	0.0197	0.0219	0.0263	0.0167	0.0178	0.0149	0.0109	0.0057	0.002	0.002	0.003	0.0119	0.0133	0.0145	0.0148
Cr	0.0010	0.0017	0.0014	0.0021	0.0023	0.0022	0.0021	0.0021	0.0008	0.0028	0.0130	0.0000	0.002	0.003	0.000	0.0022	0.0019	0.0017	0.0018
Mn	0.0128	0.0170	0.0127	0.0214	0.0194	0.0163	0.0132	0.0093	0.0084	0.0107	0.0102	0.0120	0.011	0.012	0.010	0.0174	0.0132	0.0130	0.0103
Fe	0.2692	0.2579	0.2343	0.2958	0.3051	0.2779	0.2538	0.2447	0.2547	0.2881	0.3244	0.2876	0.261	0.307	0.268	0.1582	0.1527	0.1344	0.1207
Co	0.0001	0.0001	0.0002	0.0005	0.0002	0.0002	0.0007	0.0000	0.0004	0.0002	0.0000	0.0004	0.000	0.000	0.000	0.0003	0.0001	0.0001	0.0002
Ni	0.0055	0.0061	0.0049	0.0050	0.0065	0.0068	0.0070	0.0049	0.0048	0.0042	0.0038	0.0019	0.004	0.004	0.003	0.0042	0.0045	0.0052	0.0042
Cu	0.0113	0.0110	0.0210	0.0252	0.0214	0.0230	0.0217	0.0210	0.0137	0.0175	0.0120	0.0150	0.008	0.010	0.010	0.0225	0.0177	0.0203	0.0159
Zn	0.1794	0.2399	0.1579	0.2156	0.1887	0.1567	0.1347	0.0957	0.0869	0.1045	0.0604	0.0755	0.055	0.065	0.051	0.1948	0.1337	0.1397	0.1062
Ga	0.0004	0.0018	0.0003	0.0003	0.0001	0.0000	0.0001	0.0000	0.0004	0.0000	0.0000	0.0000	0.000	0.000	0.000	0.0002	0.0002	0.0002	0.0001
As	0.0046	0.0053	0.0012	0.0043	0.0030	0.0035	0.0019	0.0028	0.0001	0.0005	0.0000	0.0000	0.000	0.000	0.000	0.0053	0.0026	0.0040	0.0023
Se	0.0021	0.0003	0.0003	0.0000	0.0000	0.0000	0.0000	0.0010	0.0000	0.0000	0.0007	0.0000	0.001	0.001	0.000	0.0000	0.0000	0.0000	0.0000
Br	0.0129	0.0106	0.0172	0.0172	0.0132	0.0129	0.0132	0.0110	0.0060	0.0109	0.0069	0.0000	0.006	0.007	0.000	0.0190	0.0160	0.0158	0.0144
Rb	0.0036	0.0020	0.0010	0.0011	0.0007	0.0007	0.0000	0.0009	0.0006	0.0007	0.0007	0.0001	0.001	0.000	0.000	0.0014	0.0006	0.0005	0.0001
Sr	0.0013	0.0011	0.0017	0.0030	0.0018	0.0020	0.0008	0.0018	0.0010	0.0006	0.0026	0.0012	0.002	0.002	0.001	0.0030	0.0016	0.0020	0.0007
Y	0.0001	0.0004	0.0003	0.0002	0.0001	0.0001	0.0001	0.0003	0.0001	0.0000	0.0002	0.0001	0.000	0.000	0.000	0.0004	0.0000	0.0001	0.0001
Zr	0.0006	0.0016	0.0010	0.0006	0.0014	0.0004	0.0005	0.0013	0.0004	0.0012	0.0021	0.0001	0.001	0.002	0.000	0.0003	0.0006	0.0006	0.0006
Mo	0.0005	0.0015	0.0007	0.0016	0.0001	0.0000	0.0021	0.0011	0.0026	0.0000	0.0001	0.0026	0.001	0.001	0.000	0.0011	0.0001	0.0000	0.0014
Pd	0.0012	0.0019	0.0006	0.0016	0.0000	0.0000	0.0001	0.0005	0.0003	0.0000	0.0002	0.0003	0.001	0.001	0.000	0.0023	0.0000	0.0000	0.0001
Ag	0.0011	0.0013	0.0010	0.0003	0.0000	0.0003	0.0000	0.0000	0.0001	0.0002	0.0000	0.0000	0.002	0.001	0.000	0.0003	0.0003	0.0002	0.0000
Cd	0.0019	0.0022	0.0008	0.0006	0.0007	0.0002	0.0005	0.0004	0.0005	0.0003	0.0001	0.0004	0.001	0.001	0.000	0.0005	0.0007	0.0005	0.0001
In	0.0018	0.0009	0.0005	0.0003	0.0001	0.0000	0.0001	0.0002	0.0004	0.0006	0.0002	0.0016	0.001	0.001	0.000	0.0005	0.0000	0.0000	0.0000
Sn	0.0188	0.0131	0.0107	0.0131	0.0041	0.0034	0.0032	0.0025	0.0055	0.0016	0.0002	0.0011	0.001	0.003	0.003	0.0125	0.0035	0.0046	0.0038
Sb	0.0046	0.0042	0.0009	0.0080	0.0005	0.0005	0.0021	0.0007	0.0008	0.0002	0.0009	0.0001	0.001	0.001	0.002	0.0068	0.0007	0.0006	0.0015
Ba	0.0267	0.0106	0.0031	0.0167	0.0348	0.0109	0.0042	0.0003	0.0194	0.0142	0.0025	0.0018	0.001	0.005	0.002	0.0087	0.0127	0.0048	0.0039
La	0.0131	0.0105	0.0036	0.0164	0.0000	0.0000	0.0040	0.0008	0.0190	0.0024	0.0034	0.0000	0.001	0.002	0.000	0.0146	0.0000	0.0000	0.0041
Au	0.0003	0.0003	0.0000	0.0000	0.0000	0.0002	0.0001	0.0001	0.0000	0.0000	0.0001	0.0000	0.001	0.000	0.000	0.0000	0.0001	0.0001	0.0000
Hg	0.0001	0.0000	0.0000	0.0000	0.0000	0.0000	0.0000	0.0000	0.0000	0.0000	0.0000	0.0000	0.000	0.000	0.000	0.0000	0.0000	0.0000	0.0000
Tl	0.0001	0.0002	0.0000	0.0000	0.0000	0.0000	0.0001	0.0000	0.0001	0.0000	0.0000	0.0000	0.000	0.000	0.000	0.0000	0.0000	0.0000	0.0002
Pb	0.0664	0.0478	0.0405	0.0597	0.0399	0.0383	0.0317	0.0182	0.0161	0.0182	0.0095	0.0118	0.007	0.008	0.006	0.0626	0.0370	0.0413	0.0344
U	0.0001	0.0013	0.0008	0.0040	0.0001	0.0000	0.0001	0.0002	0.0000	0.0000	0.0003	0.0000	0.001	0.001	0.001	0.0040	0.0000	0.0000	0.0002
Site	WB								TW										
Year	2015	2016	2017	2018	2019	2020	2021	2022	2001	2005	2009	2011	2012	2013	2014	2015	2016	2017	2018
Teflon Mass	21.082	16.985	18.665	16.720	16.652	13.201	14.940	12.610	34.122	38.593	30.612	35.298	28.644	29.503	26.194	23.835	21.500	22.378	20.726
Quartz Mass	22.370	17.098	19.317	16.849	19.021	15.002	16.187	14.463	37.280	40.748	34.003	40.558	48.255	33.966	28.663	26.344	22.915	24.746	22.113
Cl-	0.082	0.035	0.072	0.034	0.074	0.099	0.100	0.094	0.138	0.126	0.175	0.122	0.082	0.095	0.138	0.130	0.084	0.113	0.067

NO3-	0.530	0.347	0.469	0.481	0.630	0.624	0.909	0.591	1.343	1.635	2.031	1.795	1.015	1.173	0.933	1.006	0.756	0.993	1.009
SO4=	7.449	5.965	6.118	4.960	5.203	3.758	3.898	3.435	9.172	13.174	10.481	10.914	9.411	8.884	8.662	7.452	6.617	6.597	5.447
NH4+	2.398	2.157	2.123	1.743	1.941	1.196	1.280	1.302	2.965	4.070	3.268	4.385	3.403	3.359	3.046	2.625	2.438	2.415	2.060
Na+	0.454	0.211	0.376	0.284	0.319	0.316	0.321	0.282	0.397	0.362	0.211	0.404	0.306	0.292	0.398	0.379	0.307	0.371	0.284
K+	0.181	0.194	0.209	0.159	0.191	0.089	0.129	0.132	0.492	0.486	0.308	0.492	0.318	0.309	0.294	0.186	0.221	0.235	0.173
OC	2.706	3.572	3.730	1.912	2.349	1.877	2.557	2.478	8.690	6.932	4.376	5.435	4.567	4.857	5.834	4.055	5.782	5.902	3.516
EC	1.023	1.008	0.933	1.094	0.775	0.861	0.996	0.637	5.371	6.258	3.760	4.238	3.593	4.010	2.613	2.147	2.182	1.601	1.905
TC	3.725	4.581	4.663	2.965	3.123	2.712	3.523	3.077	14.041	13.181	8.124	9.649	8.160	8.859	8.447	6.197	7.964	7.503	5.379
Al	0.0943	0.1117	0.1348	0.1084	0.1250	0.038	0.078	0.085	0.1146	0.1414	0.0828	0.1910	0.2118	0.1916	0.1676	0.0864	0.1190	0.1399	0.1002
Si	0.1577	0.1739	0.2369	0.1986	0.2509	0.140	0.215	0.181	0.3870	0.3141	0.1853	0.3888	0.3899	0.3436	0.2728	0.1572	0.1875	0.2474	0.1854
P	0.0000	0.0017	0.0025	0.0000	0.0005	0.000	0.000	0.000	0.0050	0.1950	0.0237	0.0163	0.0138	0.0140	0.0157	0.0000	0.0023	0.0030	0.0000
S	2.8453	2.3997	2.4413	1.9935	2.1624	1.398	1.386	1.464	3.3789	4.5835	3.4305	3.7641	3.1509	3.1369	3.0678	2.8011	2.5678	2.5679	2.1251
Cl	0.0739	0.0440	0.1047	0.0689	0.0570	0.081	0.091	0.083	0.0874	0.0758	0.0568	0.0640	0.0491	0.0741	0.0947	0.0563	0.0501	0.1232	0.0780
K	0.2297	0.2221	0.2672	0.2041	0.2540	0.158	0.215	0.184	0.5858	0.5080	0.3281	0.4797	0.3211	0.3622	0.3194	0.2363	0.2461	0.2909	0.2132
Ca	0.0752	0.0518	0.0769	0.0902	0.0639	0.062	0.081	0.054	0.1262	0.0896	0.0729	0.1006	0.1253	0.1053	0.0993	0.0932	0.0758	0.1048	0.1043
Ti	0.0079	0.0058	0.0072	0.0098	0.0065	0.005	0.008	0.006	0.0088	0.0102	0.0084	0.0117	0.0127	0.0106	0.0093	0.0081	0.0074	0.0085	0.0106
V	0.0131	0.0144	0.0122	0.0088	0.0052	0.001	0.002	0.002	0.0137	0.0237	0.0182	0.0206	0.0208	0.0245	0.0258	0.0228	0.0213	0.0157	0.0138
Cr	0.0015	0.0005	0.0015	0.0028	0.0000	0.001	0.002	0.000	0.0009	0.0015	0.0012	0.0021	0.0022	0.0017	0.0021	0.0019	0.0003	0.0018	0.0062
Mn	0.0073	0.0048	0.0074	0.0071	0.0072	0.007	0.009	0.006	0.0124	0.0158	0.0113	0.0186	0.0163	0.0156	0.0155	0.0094	0.0071	0.0104	0.0091
Fe	0.1110	0.0822	0.1154	0.1366	0.1046	0.099	0.131	0.088	0.1871	0.1858	0.1325	0.1932	0.1962	0.1780	0.1802	0.1626	0.1467	0.1760	0.2004
Co	0.0000	0.0001	0.0000	0.0000	0.0001	0.000	0.000	0.000	0.0001	0.0001	0.0002	0.0003	0.0001	0.0001	0.0002	0.0000	0.0002	0.0001	0.0000
Ni	0.0042	0.0038	0.0037	0.0031	0.0017	0.002	0.003	0.002	0.0054	0.0071	0.0052	0.0064	0.0113	0.0073	0.0068	0.0065	0.0056	0.0044	0.0046
Cu	0.0101	0.0106	0.0153	0.0096	0.0076	0.003	0.007	0.007	0.0090	0.0104	0.0188	0.0207	0.0151	0.0212	0.0182	0.0123	0.0092	0.0117	0.0081
Zn	0.0741	0.0572	0.0761	0.0428	0.0404	0.030	0.037	0.027	0.1743	0.2186	0.1343	0.1936	0.1704	0.1501	0.2017	0.0828	0.0758	0.1175	0.0743
Ga	0.0000	0.0001	0.0002	0.0000	0.0000	0.000	0.000	0.000	0.0004	0.0030	0.0004	0.0001	0.0000	0.0000	0.0001	0.0000	0.0001	0.0003	0.0000
As	0.0035	0.0002	0.0007	0.0000	0.0000	0.000	0.000	0.000	0.0055	0.0063	0.0010	0.0046	0.0029	0.0038	0.0020	0.0027	0.0002	0.0005	0.0000
Se	0.0010	0.0000	0.0000	0.0010	0.0000	0.001	0.001	0.000	0.0022	0.0004	0.0004	0.0000	0.0001	0.0000	0.0000	0.0009	0.0000	0.0000	0.0009
Br	0.0127	0.0056	0.0112	0.0064	0.0000	0.005	0.006	0.000	0.0127	0.0099	0.0148	0.0156	0.0108	0.0128	0.0115	0.0104	0.0059	0.0096	0.0068
Rb	0.0008	0.0004	0.0003	0.0007	0.0002	0.001	0.001	0.000	0.0043	0.0025	0.0011	0.0014	0.0006	0.0006	0.0003	0.0009	0.0006	0.0004	0.0007
Sr	0.0019	0.0010	0.0007	0.0025	0.0009	0.001	0.002	0.001	0.0011	0.0011	0.0019	0.0029	0.0015	0.0015	0.0007	0.0017	0.0009	0.0006	0.0021
Y	0.0003	0.0001	0.0000	0.0002	0.0000	0.000	0.000	0.000	0.0001	0.0004	0.0004	0.0003	0.0001	0.0001	0.0001	0.0004	0.0001	0.0000	0.0002
Zr	0.0007	0.0002	0.0007	0.0009	0.0001	0.001	0.002	0.000	0.0006	0.0013	0.0008	0.0004	0.0005	0.0007	0.0008	0.0008	0.0005	0.0003	0.0013
Mo	0.0005	0.0015	0.0000	0.0002	0.0009	0.000	0.001	0.000	0.0005	0.0011	0.0006	0.0013	0.0002	0.0000	0.0018	0.0007	0.0011	0.0000	0.0003
Pd	0.0002	0.0001	0.0000	0.0001	0.0001	0.001	0.001	0.000	0.0017	0.0014	0.0007	0.0019	0.0000	0.0000	0.0001	0.0004	0.0009	0.0000	0.0002
Ag	0.0001	0.0001	0.0004	0.0001	0.0001	0.002	0.002	0.000	0.0017	0.0020	0.0007	0.0001	0.0004	0.0002	0.0000	0.0002	0.0000	0.0002	0.0001
Cd	0.0004	0.0002	0.0000	0.0003	0.0003	0.001	0.001	0.000	0.0023	0.0021	0.0007	0.0004	0.0010	0.0006	0.0001	0.0005	0.0005	0.0004	0.0002
In	0.0001	0.0003	0.0007	0.0001	0.0023	0.001	0.001	0.000	0.0020	0.0010	0.0005	0.0003	0.0000	0.0000	0.0000	0.0001	0.0006	0.0005	0.0002
Sn	0.0017	0.0045	0.0020	0.0004	0.0012	0.001	0.002	0.002	0.0203	0.0188	0.0101	0.0120	0.0032	0.0059	0.0055	0.0027	0.0084	0.0031	0.0003
Sb	0.0005	0.0012	0.0004	0.0006	0.0000	0.001	0.001	0.002	0.0049	0.0027	0.0009	0.0067	0.0002	0.0007	0.0003	0.0003	0.0017	0.0006	0.0008
Ba	0.0005	0.0150	0.0065	0.0011	0.0015	0.000	0.005	0.001	0.0170	0.0081	0.0031	0.0101	0.0115	0.0060	0.0045	0.0002	0.0160	0.0094	0.0007
La	0.0014	0.0137	0.0013	0.0033	0.0007	0.000	0.002	0.000	0.0087	0.0081	0.0034	0.0132	0.0000	0.0000	0.0042	0.0009	0.0126	0.0025	0.0020
Au	0.0001	0.0000	0.0000	0.0001	0.0000	0.000	0.001	0.000	0.0005	0.0006	0.0000	0.0000	0.0002	0.0001	0.0000	0.0002	0.0000	0.0000	0.0001
Hg	0.0001	0.0000	0.0000	0.0000	0.0000	0.000	0.000	0.000	0.0002	0.0003	0.0000	0.0000	0.0000	0.0000	0.0000	0.0000	0.0000	0.0000	0.0000
Tl	0.0000	0.0000	0.0000	0.0001	0.0000	0.000	0.000	0.000	0.0001	0.0001	0.0001	0.0000	0.0000	0.0000	0.0001	0.0000	0.0000	0.0000	0.0000
Pb	0.0181	0.0173	0.0189	0.0096	0.0112	0.006	0.007	0.007	0.0726	0.0498	0.0406	0.0599	0.0346	0.0374	0.0312	0.0182	0.0163	0.0182	0.0103
U	0.0002	0.0000	0.0000	0.0003	0.0001	0.001	0.001	0.000	0.0002	0.0011	0.0007	0.0038	0.0001	0.0000	0.0000	0.0001	0.0000	0.0002	0.0002

Site	TW				YL														KC
Year	2019	2020	2021	2022	2005	2009	2011	2012	2013	2014	2015	2016	2017	2018	2019	2020	2021	2022	2015
Teflon Mass	17.823	15.429	17.575	14.670	41.310	31.781	38.220	30.153	31.014	27.290	25.015	23.097	22.498	22.378	22.062	16.539	17.018	15.036	24.458
Quartz Mass	20.731	17.409	19.309	17.134	43.908	36.343	42.895	50.229	35.369	29.796	26.700	23.962	24.211	22.258	25.195	19.323	19.898	17.325	26.557
Cl-	0.073	0.092	0.099	0.116	0.264	0.213	0.174	0.131	0.111	0.142	0.093	0.104	0.107	0.090	0.083	0.091	0.086	0.091	0.098
NO3-	0.859	0.684	1.427	0.889	2.864	2.419	2.590	1.434	1.761	1.431	1.429	1.161	1.213	1.624	1.426	1.030	1.689	0.977	0.848
SO4=	5.072	3.825	3.944	3.503	13.910	11.041	10.851	9.583	8.964	8.625	7.283	6.659	6.516	5.425	5.722	4.056	3.870	3.384	7.737
NH4+	1.987	1.218	1.430	1.382	4.617	3.470	4.627	3.556	3.540	3.292	2.714	2.574	2.515	2.322	2.370	1.387	1.515	1.411	2.679
Na+	0.330	0.306	0.338	0.333	0.375	0.262	0.402	0.323	0.278	0.352	0.344	0.274	0.322	0.243	0.280	0.272	0.295	0.275	0.364
K+	0.167	0.093	0.137	0.139	0.562	0.365	0.590	0.374	0.385	0.348	0.234	0.298	0.260	0.219	0.248	0.126	0.151	0.151	0.185

OC	3.568	3.170	3.493	3.721	7.235	4.834	5.727	4.689	5.023	6.147	4.244	5.851	5.291	3.516	4.414	3.137	3.595	3.716	4.055
EC	1.284	1.380	1.528	1.146	6.194	3.488	4.606	3.604	3.959	2.572	2.037	2.220	1.702	2.099	1.547	1.439	1.501	1.082	2.760
TC	4.853	4.541	4.991	4.827	13.420	8.310	10.309	8.294	8.974	8.719	6.277	8.071	6.993	5.574	5.962	4.550	5.066	4.758	6.810
Al	0.0941	0.030	0.072	0.093	0.1448	0.0913	0.2114	0.2368	0.2115	0.1784	0.0903	0.1299	0.1389	0.1053	0.1405	0.039	0.088	0.100	0.0768
Si	0.1831	0.125	0.193	0.189	0.3221	0.2073	0.4349	0.4311	0.3779	0.2897	0.1726	0.2040	0.2413	0.1964	0.2913	0.144	0.228	0.215	0.1544
P	0.0003	0.001	0.000	0.000	0.1917	0.0229	0.0155	0.0148	0.0145	0.0137	0.0000	0.0020	0.0022	0.0000	0.0004	0.001	0.000	0.000	0.0000
S	2.1103	1.471	1.449	1.496	4.5622	3.4535	3.7813	3.2280	3.0990	3.0908	2.7812	2.5303	2.5762	2.1353	2.2856	1.499	1.302	1.421	2.9326
Cl	0.0796	0.084	0.083	0.095	0.1590	0.0941	0.0774	0.0621	0.0788	0.0941	0.0683	0.0640	0.0917	0.0787	0.0566	0.071	0.074	0.080	0.0444
K	0.2098	0.156	0.223	0.199	0.5631	0.3828	0.5722	0.3882	0.4366	0.3839	0.2850	0.3290	0.3227	0.2509	0.3211	0.198	0.230	0.213	0.2270
Ca	0.0662	0.076	0.086	0.072	0.0891	0.0738	0.1111	0.1207	0.1088	0.0935	0.0938	0.0802	0.0878	0.1046	0.0882	0.070	0.101	0.078	0.0920
Ti	0.0056	0.006	0.009	0.008	0.0114	0.0097	0.0156	0.0153	0.0139	0.0108	0.0093	0.0093	0.0117	0.0125	0.0101	0.007	0.012	0.009	0.0080
V	0.0061	0.002	0.002	0.003	0.0195	0.0144	0.0139	0.0145	0.0142	0.0176	0.0147	0.0160	0.0132	0.0100	0.0046	0.001	0.001	0.002	0.0370
Cr	0.0000	0.002	0.002	0.000	0.0017	0.0016	0.0024	0.0022	0.0020	0.0023	0.0021	0.0003	0.0017	0.0060	0.0000	0.001	0.003	0.000	0.0017
Mn	0.0063	0.009	0.010	0.008	0.0170	0.0127	0.0215	0.0190	0.0183	0.0140	0.0102	0.0102	0.0103	0.0110	0.0124	0.011	0.011	0.010	0.0091
Fe	0.1358	0.147	0.171	0.135	0.1996	0.1552	0.2215	0.2223	0.2027	0.1877	0.1752	0.1657	0.1785	0.2166	0.1991	0.163	0.193	0.157	0.1851
Co	0.0002	0.000	0.000	0.000	0.0001	0.0001	0.0004	0.0001	0.0000	0.0003	0.0000	0.0002	0.0001	0.0000	0.0003	0.000	0.000	0.000	0.0000
Ni	0.0021	0.003	0.004	0.003	0.0068	0.0044	0.0049	0.0051	0.0049	0.0051	0.0045	0.0041	0.0037	0.0035	0.0016	0.003	0.003	0.002	0.0104
Cu	0.0063	0.005	0.005	0.005	0.0113	0.0167	0.0234	0.0167	0.0378	0.0321	0.0127	0.0110	0.0112	0.0085	0.0091	0.005	0.007	0.005	0.0164
Zn	0.0506	0.045	0.050	0.037	0.2381	0.1600	0.2188	0.1879	0.1515	0.1183	0.1052	0.0963	0.0782	0.0730	0.0696	0.078	0.052	0.044	0.0780
Ga	0.0000	0.000	0.000	0.000	0.0024	0.0003	0.0001	0.0002	0.0001	0.0000	0.0000	0.0001	0.0002	0.0000	0.0000	0.000	0.000	0.000	0.0000
As	0.0000	0.000	0.000	0.000	0.0084	0.0016	0.0058	0.0029	0.0044	0.0022	0.0035	0.0005	0.0004	0.0001	0.0000	0.000	0.000	0.000	0.0029
Se	0.0000	0.001	0.001	0.000	0.0005	0.0004	0.0000	0.0000	0.0001	0.0000	0.0010	0.0000	0.0000	0.0007	0.0000	0.001	0.001	0.000	0.0010
Br	0.0000	0.005	0.007	0.000	0.0116	0.0143	0.0171	0.0122	0.0133	0.0123	0.0105	0.0060	0.0089	0.0070	0.0016	0.005	0.006	0.000	0.0105
Rb	0.0002	0.001	0.001	0.000	0.0029	0.0015	0.0016	0.0010	0.0008	0.0005	0.0012	0.0008	0.0007	0.0010	0.0003	0.001	0.001	0.000	0.0008
Sr	0.0007	0.001	0.002	0.001	0.0015	0.0020	0.0030	0.0014	0.0017	0.0006	0.0017	0.0013	0.0008	0.0023	0.0008	0.002	0.002	0.001	0.0017
Y	0.0001	0.000	0.000	0.000	0.0004	0.0003	0.0004	0.0001	0.0001	0.0001	0.0002	0.0002	0.0000	0.0003	0.0000	0.000	0.000	0.000	0.0004
Zr	0.0000	0.001	0.002	0.000	0.0007	0.0011	0.0006	0.0007	0.0006	0.0011	0.0010	0.0004	0.0010	0.0014	0.0002	0.001	0.002	0.000	0.0009
Mo	0.0016	0.000	0.001	0.001	0.0017	0.0007	0.0009	0.0001	0.0000	0.0027	0.0007	0.0015	0.0000	0.0003	0.0015	0.000	0.001	0.000	0.0010
Pd	0.0002	0.001	0.001	0.001	0.0016	0.0008	0.0018	0.0000	0.0000	0.0001	0.0003	0.0005	0.0000	0.0001	0.0002	0.000	0.001	0.000	0.0002
Ag	0.0001	0.002	0.002	0.000	0.0018	0.0008	0.0001	0.0002	0.0003	0.0000	0.0001	0.0001	0.0001	0.0001	0.0000	0.002	0.002	0.000	0.0001
Cd	0.0005	0.000	0.001	0.000	0.0025	0.0007	0.0007	0.0008	0.0004	0.0005	0.0003	0.0003	0.0003	0.0001	0.0003	0.001	0.001	0.000	0.0003
In	0.0018	0.001	0.000	0.000	0.0017	0.0005	0.0002	0.0001	0.0000	0.0000	0.0001	0.0005	0.0006	0.0002	0.0011	0.001	0.001	0.000	0.0002
Sn	0.0015	0.001	0.001	0.002	0.0162	0.0100	0.0154	0.0049	0.0113	0.0076	0.0026	0.0081	0.0012	0.0004	0.0026	0.001	0.003	0.003	0.0021
Sb	0.0000	0.001	0.001	0.002	0.0039	0.0014	0.0087	0.0004	0.0009	0.0021	0.0005	0.0012	0.0005	0.0006	0.0002	0.000	0.001	0.002	0.0009
Ba	0.0000	0.001	0.004	0.001	0.0068	0.0024	0.0108	0.0205	0.0119	0.0056	0.0005	0.0139	0.0087	0.0006	0.0000	0.001	0.005	0.000	0.0004
La	0.0000	0.001	0.002	0.000	0.0082	0.0040	0.0165	0.0000	0.0000	0.0061	0.0014	0.0107	0.0026	0.0013	0.0000	0.001	0.002	0.000	0.0007
Au	0.0000	0.001	0.000	0.000	0.0002	0.0001	0.0000	0.0001	0.0002	0.0001	0.0002	0.0000	0.0001	0.0001	0.0000	0.001	0.000	0.000	0.0001
Hg	0.0000	0.000	0.000	0.000	0.0001	0.0000	0.0000	0.0000	0.0000	0.0000	0.0000	0.0000	0.0000	0.0000	0.0006	0.000	0.000	0.000	0.0001
Tl	0.0000	0.000	0.000	0.000	0.0000	0.0001	0.0000	0.0000	0.0000	0.0001	0.0000	0.0001	0.0000	0.0001	0.0000	0.000	0.000	0.000	0.0000
Pb	0.0086	0.008	0.008	0.007	0.0624	0.0437	0.0671	0.0384	0.0428	0.0356	0.0210	0.0205	0.0184	0.0121	0.0132	0.009	0.008	0.007	0.0177
U	0.0000	0.000	0.001	0.000	0.0017	0.0007	0.0035	0.0000	0.0000	0.0001	0.0002	0.0000	0.0000	0.0004	0.0000	0.001	0.001	0.001	0.0002

Site	KC						
Year	2016	2017	2018	2019	2020	2021	2022
Teflon Mass	20.740	22.076	19.512	18.893	15.312	16.812	14.669
Quartz Mass	22.106	23.913	20.775	21.987	17.406	18.701	16.832
Cl-	0.072	0.087	0.057	0.077	0.086	0.106	0.101
NO3-	0.612	0.705	0.753	0.753	0.659	1.242	0.673
SO4=	6.557	6.511	5.285	5.357	3.887	3.960	3.506
NH4+	2.420	2.287	1.951	2.038	1.251	1.390	1.331
Na+	0.294	0.395	0.289	0.322	0.298	0.337	0.307
K+	0.220	0.233	0.158	0.180	0.093	0.128	0.132
OC	5.171	5.140	3.090	3.523	3.229	3.385	3.613
EC	2.604	2.278	2.282	1.618	1.690	1.756	1.381
TC	7.775	7.418	5.331	5.141	4.910	5.112	4.954
Al	0.1243	0.1439	0.0984	0.1134	0.032	0.068	0.093
Si	0.1905	0.2602	0.1869	0.2316	0.124	0.181	0.200

P	0.0030	0.0025	0.0000	0.0008	0.000	0.000	0.000
S	2.5521	2.5774	2.0820	2.2351	1.478	1.459	1.488
Cl	0.0518	0.1088	0.0785	0.0605	0.076	0.079	0.103
K	0.2426	0.2929	0.2016	0.2535	0.153	0.209	0.190
Ca	0.0842	0.1331	0.1086	0.0812	0.078	0.088	0.077
Ti	0.0076	0.0096	0.0114	0.0075	0.006	0.009	0.007
V	0.0252	0.0198	0.0169	0.0059	0.004	0.004	0.005
Cr	0.0002	0.0029	0.0034	0.0000	0.002	0.002	0.000
Mn	0.0065	0.0118	0.0087	0.0095	0.009	0.009	0.008
Fe	0.1715	0.2115	0.2156	0.1925	0.185	0.193	0.168
Co	0.0002	0.0001	0.0000	0.0002	0.000	0.000	0.000
Ni	0.0062	0.0054	0.0053	0.0026	0.005	0.007	0.005
Cu	0.0162	0.0175	0.0105	0.0089	0.005	0.005	0.006
Zn	0.0764	0.0832	0.0593	0.0675	0.044	0.058	0.036
Ga	0.0000	0.0001	0.0000	0.0000	0.000	0.000	0.000
As	0.0002	0.0004	0.0000	0.0000	0.000	0.000	0.000
Se	0.0000	0.0000	0.0008	0.0000	0.001	0.001	0.000
Br	0.0053	0.0099	0.0066	0.0000	0.005	0.007	0.000
Rb	0.0005	0.0004	0.0007	0.0002	0.001	0.001	0.000
Sr	0.0009	0.0009	0.0022	0.0004	0.001	0.002	0.001
Y	0.0001	0.0000	0.0002	0.0001	0.000	0.000	0.000
Zr	0.0001	0.0010	0.0014	0.0000	0.002	0.002	0.000
Mo	0.0014	0.0000	0.0001	0.0011	0.001	0.001	0.000
Pd	0.0007	0.0000	0.0001	0.0003	0.001	0.001	0.000
Ag	0.0002	0.0000	0.0001	0.0001	0.001	0.002	0.000
Cd	0.0001	0.0003	0.0002	0.0006	0.000	0.001	0.000
In	0.0005	0.0006	0.0001	0.0011	0.001	0.001	0.000
Sn	0.0041	0.0029	0.0004	0.0011	0.001	0.002	0.002
Sb	0.0010	0.0000	0.0008	0.0000	0.000	0.001	0.002
Ba	0.0208	0.0132	0.0006	0.0000	0.001	0.004	0.001
La	0.0164	0.0005	0.0033	0.0000	0.000	0.002	0.000
Au	0.0000	0.0000	0.0001	0.0000	0.000	0.000	0.000
Hg	0.0000	0.0000	0.0000	0.0002	0.000	0.000	0.000
Tl	0.0000	0.0000	0.0000	0.0000	0.000	0.000	0.000
Pb	0.0156	0.0180	0.0096	0.0107	0.008	0.009	0.007
U	0.0000	0.0001	0.0003	0.0000	0.000	0.000	0.001